Effects of eutrophication on sedimentary organic carbon cycling in five temperate lakes

Annika Fiskal[1*], Longhui Deng[1], Anja Michel[1], Philip Eickenbusch[1], Xingguo Han[1], Lorenzo Lagostina[1], Rong Zhu[1], Michael Sander[1], Martin H. Schroth[1], Stefano M. Bernasconi[3], Nathalie Dubois[2,3], Mark A. Lever[1*]

[1] Institute of Biogeochemistry and Pollutant Dynamics (IBP), *ETH Zurich, Universitätstrasse 16, 8092 Zurich, Switzerland*
[2] Surface Waters Research – Management, Eawag, Swiss Federal Institute of Aquatic Science and Technology, Überlandstrasse 133, 8600 Dübendorf, Switzerland
[3] *Department of Earth Sciences, ETH Zurich, Sonneggstrasse 5, 8092 Zurich, Switzerland*

[*]*Correspondence to*: Annika Fiskal (annika.fiskal@usys.ethz.ch) and Mark A. Lever (mark.lever@usys.ethz.ch)

Keywords
organic carbon burial, organic carbon accumulation, temperate lake sediment, microbial respiration, phosphorus, methanogenesis, redox zonation, power model, oxygen exposure time

Abstract. Even though human induced eutrophication has severely impacted temperate lake ecosystems over the last centuries, the effects on total organic carbon (TOC) burial and mineralization are not well understood. We study these effects based on sedimentary records from the last 180 years in five Swiss lakes that differ in trophic state. We compare changes in TOC content and modeled TOC accumulation rates through time to historical data on algae blooms, water column anoxia, wastewater treatment, artificial lake ventilation, and water column phosphorus (P) concentrations. We furthermore investigate the effects of eutrophication on rates of microbial TOC mineralization and vertical distributions of microbial respiration reactions in sediments. Our results indicate that the history of eutrophication is well recorded in the sedimentary record. Overall, eutrophic lakes have higher TOC burial and accumulation rates, and subsurface peaks in TOC coincide with past periods of elevated P concentrations in lake water. Sediments of eutrophic lakes, moreover, have higher rates of total respiration and higher contributions of methanogenesis to total respiration. Yet, strong overlaps in the distributions of respiration reactions involving different electron acceptors in all lakes indicate no major effect of trophic state on the relative distributions of these reactions. Moreover, even though water column P concentrations have been reduced by ~50-90% since the period of peak eutrophication in the 1970s, TOC burial and accumulation rates have only decreased significantly, by ~20 and 25%, in two of the five lakes. Hereby there is no clear relationship between the magnitude of the P concentration decrease and the change in TOC burial and accumulation rate. Instead, data from one eutrophic lake, suggest that artificial ventilation, which has been used to prevent water column anoxia in this lake for 35 years, may help sustain high rates of TOC burial and accumulation in sediments despite strongly reduced water column P concentrations. Our study provides novel insights into the influence of human activities in lakes and lake watersheds on lake sediments as carbon sinks and habitats for diverse microbial respiration processes.

1 Introduction

Lake sediments play an important role in the global carbon cycle despite covering only about 1 % of the Earth's surface area (Cole et al., 2007; Battin et al., 2009). Estimates of global carbon dioxide (CO_2) net fluxes from lake systems range from 60 to 580 Tg C yr^{-1} (Raymond et al., 2013; Holgerson and Raymond, 2016). Methane (CH_4) fluxes are much smaller (6 to 36 Tg C; (Bastviken et al., 2004), but are also globally important given that CH_4 has a 28 to 36 times higher global warming potential than CO_2 on a timescale of about 100 years (Cubasch et al., 2014). Besides being important sources of CO_2 and CH_4, lakes are also important sinks of organic C (OC). Global storage of C in lake sediments for the entire Holocene is estimated to be ~820 Pg C (Einsele et al., 2001; Mendonca et al., 2017)

Whether OC in lake sediments is buried and preserved over geologic time or degraded to CO_2 and CH_4 is partially controlled by sediment microorganisms, which break down OC for energy conservation and biosynthesis (Nedwell, 1984). In a first step, microorganisms enzymatically hydrolyze organic macromolecules, e.g. proteins, nucleic acids, lipids and polysaccharides, extracellularly into sufficiently small components that can be taken up across the cell membrane (Canfield et al., 2005). If oxygen (O_2) is available as an electron acceptor, organisms performing initial hydrolysis are often capable of oxidizing hydrolysis products all the way to CO_2. In the absence of O_2, OC is degraded to CO_2 or CH_4 by multiple groups of more specialized microorganisms (Canfield et al., 2005). Primary fermenters carry out the initial extracellular hydrolysis, and subsequently gain energy from the intracellular disproportionation of hydrolysis products to smaller molecules such as H_2, short chain organic acids, and alcohols. In some cases, an intermediary secondary fermentation step takes place whereby the organic acids and alcohols produced by primary fermenters are disproportionated to H_2, acetate, and C_1 compounds (Capone and Kiene, 1988; Schink, 1997). The products of primary and secondary fermentation are subsequently converted to CO_2 or CH_4 by respiring organisms using - in order of energy yields from high to low - nitrate (NO_3^-), manganese(IV) (Mn(IV)), ferric iron (Fe(III)), sulfate (SO_4^{2-}), and CO_2 as electron acceptors (Froelich et al., 1979; Drake et al., 2006). The differences in energy yields can result in a vertical zonation ("redox zonation") of respiration reactions, with NO_3^- reduction (denitrification) occurring near the sediment surface, as soon as O_2 is depleted, CO_2 reduction via methanogenesis dominating in deeper layers, where all other electron acceptors have been depleted, and Mn(IV), Fe(III), and SO_4^{2-} reduction taking place in distinct sediment intervals between the zones of denitrification and methanogenesis (Lovley and Goodwin, 1988; Hoehler et al., 1998; Canfield et al., 2005; Jørgensen and Kasten, 2006; Canfield and Thamdrup, 2009).

A complex set of interacting variables determines whether microorganisms break down sedimentary organic compounds, and thus whether organic carbon is stored in sediment in the long term, or returns to the hydrosphere and atmosphere as CO_2 and methane over shorter time scales. Aerobic respiration results in the breakdown of a larger fraction of the sedimentary organic carbon pool compared to anaerobic processes (Lehmann et al., 2002; Sobek et al., 2009; Katsev and Crowe, 2015). The O_2 exposure time, i.e. the time each organic molecule is present under oxic conditions, is also positively correlated with organic matter degradation. This O_2 exposure time is affected by the presence of sediment macrofauna, which physically transport sediment from deeper anoxic layers to the surface or pump O_2 into deeper anoxic layers (Kristensen, 2000;

Meysman et al., 2006; Kristensen et al., 2012; Middelburg, 2018). Macrofauna also mineralize OC through their own feeding activities, and stimulate the microbial mineralization of organic matter by breaking large organic particulates into smaller ones with a larger surface area for microbial colonization. The chemical composition and structure of the OC also affects OC preservation. OC of terrestrial plants is typically more resistant to microbial attack than OC of phytoplankton due to presence of biologically resistant polymers, e.g. lignin, waxes, resins, that are absent in phytoplankton (Burdige, 2007). Abiotic processes, e.g. condensation reactions (e.g. Burdige, 2007), incorporation of sedimentary Fe(III) (Lalonde et al., 2012) or sulfur compounds (Werne et al., 2000; Hebting et al., 2006; Werne et al., 2008), and physical protection by adsorption or encapsulation can also significantly decrease rates of microbial OC degradation (reviewed in (Hedges et al., 2000)).

Besides these natural factors, the burial of C in lake sediment is also largely influenced by anthropogenic activities, such as agriculture, wastewater input, and urbanization (Heathcote and Downing, 2012; Anderson et al., 2013). OC burial rates may increase due to increased water column primary production resulting from increased nutrient input, especially P (Dean and Gorham, 1998; Maerki et al., 2009; Heathcote and Downing, 2012; Anderson et al., 2013; Anderson et al., 2014), which is the limiting nutrient for primary production in most lake water columns (Correll, 1999; Conley et al., 2009). Hereby increased OC loading due to stimulation of primary production (eutrophication) enhances OC sedimentation rates and microbial O_2 consumption (Valiela et al., 1997; Gontikaki et al., 2012). The resulting (seasonal) water column hypoxia or anoxia negatively impact ecosystem functioning, as well as commercial and recreational uses (Valiela et al., 1997; McGlathery, 2001; Breitburg, 2002). Strategies to manage eutrophication include restrictions in terrestrial P use, agriculture-free buffer zones, wastewater treatment with P precipitation systems, and artificial water column mixing and aeration (Schindler, 2006; Conley et al., 2009). These remediation strategies can lead to substantial reductions in P concentrations in lake water (Müller et al., 1990; Liechti, 1994). Yet, there are still open questions regarding the influence of these mitigation strategies on OC burial, in part due to P retention and release from lake sediments (Gachter and Muller, 2003; Moosmann et al., 2006). Furthermore, links between historically documented human activities in lakes and lake watersheds, eutrophication in lake water columns, which would inform on links between OC burial and mineralization processes in lake sediments.

Here we investigate OC burial through time as well as OC mineralization rates across five temperate lakes that differ in eutrophication history over the past 180 years. We combine historical P concentration data with reconstructed past OC inputs (accumulation rates) to sediments and additionally investigate the effects of eutrophication on TOC mineralization rates, the distribution of microbial respiration reactions, and microbial cell abundance. We test the hypothesis that *(i)* OC burial rates have historically increased in response to anthropogenic eutrophication, and that *(ii)* increased P concentrations, and its effects on water column primary production and O_2 concentrations, are the main driver of this increased OC burial. We furthermore test the hypothesis that increased energy supplies due to higher OC availability in eutrophic lake sediments result in *(iii)* higher microbial respiration rates, *(iv)* changes in the vertical zonation and relative contributions of dominant respiration reactions, and (*v*) increases in both microbial population size and cell-specific C turnover. Our results indicate that anthropogenic eutrophication during the latter half of the 20th century, which was largely driven by anthropogenic wastewater inputs, indeed increased OC burial and OC respiration rates, especially methanogenesis rates, as well as cell-specific microbial C turnover.

Yet, we observe no clear impact of eutrophication on the zonation of microbial respiration reactions relative to each other, or on microbial population size. Furthermore, despite strong decreases in water column P concentrations in recent years, TOC burial rates remain clearly elevated. To our knowledge, this is the first study to provide a detailed historic record and reconstruction of how recent human activities that have driven water column eutrophication have impacted OC burial, OC mineralization rates, and the distributions of microbial respiration reactions in lacustrine sediments.

2 Material and Methods

2.1 Study sites & their eutrophication history

We sampled sediments from three water depths in five lakes in central Switzerland: Lake Lucerne, Lake Zurich, Lake Zug, Lake Baldegg, and Lake Greifen (Fig. S1). All five lakes undergo strong seasonal changes in primary production, thermal stratification, and sedimentation (Teranes et al., 1999a; Teranes et al., 1999b; Buergi and Stadelmann, 2000; Naeher et al., 2013), but differ in land use and in histories of anthropogenic eutrophication and eutrophication mitigation (Fig.1, for further info see Fig. S2, SI Text 1 "Extended Lake description"). Based on total P concentrations in surface water today, Lake Lucerne is oligotrophic, Lake Zurich is mesotrophic, and the other three lakes are all highly eutrophic.

Over the past 180 years, these five lakes show similar, but distinct trends in eutrophication history (Fig. 1). In Lake Baldegg, strong P concentration increases coinciding with algal blooms and water column anoxia already started around 1890. Similarly dramatic changes occurred in Lake Greifen from 1920 onwards, and to a lesser extent in Lake Zug starting in the 1930s. For Lake Zurich no reconstructed P concentrations are available, however, measured concentrations indicate relatively low and steady P levels from 1950 to 1960, followed by an increase from thereon. In Lake Lucerne reconstructed P concentrations indicate low and relatively steady concentrations until a small, temporary increase started in the 1960s.

In all five lakes, the strongest increases in P concentrations occurred between ~1950–1970, yet, the magnitude of these increases differed (Fig. 1). Annual P concentration maxima in Lake Greifen (16.1 µM, 1969) and Lake Baldegg (15.4 µM, 1969) were ~2.5 fold higher than in Lake Zug (6.6 µM, 1980), ~5 fold higher than in Lake Zurich (3.3 µM, 1973), and ~9 fold higher than in Lake Lucerne (1.7 µM, 1973). Since then, remediation measures, such as wastewater treatment, and P detergent bans have strongly decreased water column P concentrations.

2.2 Sampling

All took place in June and July of 2016. Three sublittoral stations differing in water depth and bottom water O_2 concentrations were sampled (Table 1). All sites were bioturbated, based on presence of infaunal chironomid larvae and/or oligochaete worms, except the deepest station in the hypoxic basin of Lake Zurich (137 m water depth).

Per each lake station, one 60-mm diameter and 3–4 150-mm diameter gravity cores (UWITEC, AT) were taken from boats or motorized platforms. The thin cores were used for analyses of radionuclides, X-ray fluorescence, grain size, and archiving (one-half) (for core photos see SI Fig. S3). Wide cores underwent a brief lithostratigraphic description and were then

used as follows: the core with the least disturbed sediment surface was used for microsensor measurements (O_2, pH). Sediment porewater samples were obtained by rhizons (0.2 µm pore size, Rhizosphere) from a designated core with pre-drilled holes that were taped during coring. The initial dead spaces of syringes, stop cocks and rhizons were flushed twice with the first 2–3 mL of porewater to remove any air (O_2), enabling anoxic sampling. The porewater was then sampled for downstream analyses

5   on dissolved anions and cations including redox sensitive elements, such as dissolved iron (Fe^{2+}) and hydrogen sulfide (HS^-). Sediment samples for cell counts, methane concentration analyses, and physical property determinations (porosity, bulk density, dry density, water content) were taken from a third core using sterile cut-off syringes. Samples for solid-phase carbon analyses (TOC, total inorganic carbon (TIC)) were also taken from this core. Macrofauna was collected by sieving a fourth core or the core previously used for microsensor analyses through 400 and 200 µm meshed sieves, and preserved in 70 %

10   ethanol.

2.3 Analyses

Microsensor analyses. To determine the distribution of aerobic microbial activity and pH conditions in surface sediments, triplicated depth profiles of dissolved [O_2] and pH were measured with 100-µm Clark-type microelectrodes using a field multimeter system and micromanipulator (Unisense, DK). Cores were fixed in tall plastic boxes that had been filled with lake

15   water and maintained at their original temperatures, which had been measured immediately after core retrieval. Measurements were performed as soon as possible after retrieval. Overlying water was gently bubbled with air throughout the measurements to prevent establishment of anoxic conditions. Therefore O_2 profiles in overlying water do not accurately reflect *in situ* concentrations. By contrast, O_2 concentrations in sediments were not altered by bubbling, as indicated by a high degree of reproducibility in O_2 gradients during three successive measurements.

[Fe^{2+}] and [Mn^{2+}]. Porewater concentration profiles of Fe^{2+} and Mn^{2+} were measured to determine the distributions of microbial Fe and Mn reduction. 3–5 ml of porewater were fixed with 50 µl of 30 % HCl and kept at 4°C until measurement by Inductively Coupled Plasma-Optical Emission Spectroscopy (ICP-OES) (5100, Agilent Technologies) after dilution with Milli-Q water. Standards were made using ICP-multi element standards (solution IV, MERCK, Certipur). Dissolved Fe^{2+} was

25   also determined spectrophotometrically (Plate Reader Biotek, Synergy HT) at 562 nm absorption using a ferrozine assay (Stookey, 1970; Braunschweig et al., 2012). Standards were made from $FeCl_2$ (Sigma, analytical quality) and verified using ICP-OES. Both methods show good general agreement (Fig. S4), however, values obtained by spectrophotometry were often slightly lower than those measured by ICP-OES. Tests involving different ferrozine concentrations, spiked samples, and various centrifugation treatments showed that ICP-OES data were less prone to matrix effects and overall more robust. We

30   thus only discuss the Fe^{2+} data measured by ICP-OES from here on.

[HS^-]. Porewater concentrations of HS- were measured to detect sulfate-reducing microbial activity and potential coupling between microbial sulfate and metal reduction. 1 ml of porewater was fixed with 1 ml of 5 % zinc acetate and frozen at -20°C

until photometric determination on a plate reader (Synergy HT, BioTek) with diamine reagent (methylene blue method (Cline, 1969)). Standards were prepared from a zinc sulfide stock solution made from sodium sulfide diluted in 1 % zinc acetate solution under precipitation of zinc sulfide. HS^- concentrations were then determined by titration with 25 mM sodium thiosulfate.

Inorganic ions. Concentrations of the inorganic anions (sulfate (SO_4^{2-}) and nitrate (NO_3^-)), and the cations ammonium (NH_4^+) were quantified to determine the distribution of microbial sulfate reduction and N cycling (denitrification, breakdown of N-containing organic matter). For each analysis 3 ml of porewater were sampled. 5 µl of NaOH (2M) and 5 µl HCl (2M) were added for anion and cation analyses, respectively, to increase or lower the pH by 2–3 units. Samples were kept on ice in the field and frozen at -20 °C until measurement by Ion chromatography (DIONEX DX-320 for Anions, DX-ICS-1000 for Cations). Standards were prepared by dissolving analytical quality sodium nitrate, sodium sulfate, and ammonium chloride in Milli-Q water. The DX-320 was equipped with a AERS 500, a 4-mm suppressor, a guard column (AG11-HC), and a main column (AS11-HC). The eluent, potassium hydroxide (10 mM), was generated by an eluent generator cartridge. The DX-ICS-1000 was equipped with an SCRS Ultra II, a 4-mm suppressor, a CG 12 A guard column, and a CS 12 A main column. The eluent used was methanosulfonic acid (20 mM) and prepared fresh on every measurement day.

Dissolved inorganic carbon (DIC). DIC concentration profiles were measured to determine distribution and rates of OC mineralization. Porewater was filled headspace-free into 1.5 ml borosilicate vials and stored at 4°C for up to 4 weeks. Samples were analyzed along with standards, produced by dissolving sodium bicarbonate in Milli-Q, on a GasBench II (Thermo Fisher Delat V and TC/EA) coupled to MS after acidification with 85 % phosphoric acid.

[CH_4]. Concentration profiles of CH_4 were measured to determine the distribution and rates of microbial methanogenesis. 2 cm^3 of sediment were transferred to 20-ml crimp vials containing 2.51 g NaCl and 5 ml Milli-Q water, crimped, thoroughly homogenized by shaking, and stored on ice until analysis by Gas Chromatography (GC). The GC was equipped with an autosampler (PAL GC-xt, CTC Analytics AG) and a Flame Ionization Detector (FID) (Thermo Scientific™ TRACE™ Ultra Gas Chromatograph). The working conditions for the measurement were: prep flow 10 pounds per square inch (psi), GC flow 14 psi, and CO_2 reference gas 25 psi.

Solid-phase iron pools. For extraction of biologically available particulate Fe(II) and Fe(III), 2 cm^3 of sediment were transferred to 20-ml crimp vials, immediately flushed with N_2, and stored cool at 4°C until measurement. Extraction from 0.2–0.6 g of wet sediment was performed with 5 ml 0.5 M HCl. The extract was split into two subsamples. To determine Fe(II), 40 µl of extract were mixed with 2 ml of 0.02 % ferrozine in 50 mM HEPES at pH 7 (Stookey, 1970; Lovley and Phillips, 1987) and then quantified photometrically on a Plate Reader (Synergy HT, BioTek). For total Fe, 1 ml of extract was mixed

with 0.2 ml hydroxylamine (1.5 M) to reduce Fe(III) to Fe(II) and then measured as above. Fe(III) concentrations were the difference of total Fe and Fe(II). Standards consisted of dilution series of 100 ml 100 mM $FeSO_4$ in 0.5 M HCl.

Redox state of sediment. Total electron accepting and donating capacities of the sediment were determined by mediated electrochemical reduction and oxidation, respectively (Kluepfel et al., 2014; Klupfel et al., 2014; Sander et al., 2015). Samples were treated as for solid-phase Fe extraction and analyzed inside an anoxic glove box. Before measurement, each sample was diluted into a slurry by adding 10 ml of O_2-free Milli-Q water. Further details can be found in the SI Text "Detailed description of redox state analysis of the sediment".

TOC. TOC was measured to determine OC accumulation and burial over time. 5–10 g of frozen sediment was freeze-dried in glass vials, homogenized, and split into three subsamples. One subsample was decarbonized with 6 M HCl, oven-dried, and homogenized for TOC analyses with an elemental analyzer (Thermo Fisher Flash EA 1112) coupled to an isotope-ratio-mass spectrometer (Thermo Fisher Delta V Plus) (EA-IRMS). The second subsample was analyzed directly by EA-IRMS to determine Total Carbon (TC) content in order to calculate TOC as the difference of TC minus TIC. Standards consisted of known amounts of peptone, atropine, and nicotinamide. The third subsample was used to determine TIC by coulometry (5011 CO_2 Coulometer). Some TC measurements could not be used due to high sulfur contents in the samples; therefore, TOC was back-calculated from TOC of the decarbonized fraction using an acidification factor derived from TIC measurements for all samples. To check that these calculations were correct, TOC was also calculated as the difference between TC minus TIC for those samples where TC measurements were available. All TOC data were expressed in weight % (wt. %) of dry sediment.

Cell counts. Cell counts were performed on 0.5 cm^3 of sediment after cell extraction by combined sonication and fluoric acid treatment followed by flow cytometric quantification after the method of Deng et al. (2019).

Physical Properties Analyses. Porosity, water content, bulk density, and dry density of sediment samples were determined by weighing 2 cm^3 of wet sample before and after oven drying at 60°C for at least 48 h.

Determination of sedimentation rates. Analyses of unsupported ^{210}Pb (half-life: 22.3 years) and ^{137}Cs (30.2 years) were performed by gamma spectroscopy on 2–20 g of dry sediment subsamples on a High-purity Germanium well detector. Calibrations were performed using the National Institute of Standards and Technology NG7 standard (246 kBq). Raw data were processed using the software GENIE2K 3.2.1. Sedimentation rates based on ^{210}Pb were calculated according to Binford (1990). Sedimentation rates ^{137}Cs (cm yr^{-1}) were calculated using the distinct peaks from bomb testings (1954, 1963) and the Chernobyl accident (1986). Surface sediments were assigned the year 2016, as confirmed by the short-lived radionuclide Beryllium-7 (half-life: 53.3 days). Sedimentation rate estimates based on ^{137}Cs and ^{210}Pb were similar throughout the dataset (the coefficient of variation for all stations was <10%, the mean coefficient of variation was ~3%). However in a few cases, i.e. Lake Lucerne stations 1 and 2, Lake Baldegg station 3, ^{210}Pb profiles scattered more than ^{137}Cs. Thus, in Lake Baldegg,

varve counting was used for additional verification, and showed good agreement with rates based on ^{210}Pb and ^{137}Cs. Sedimentation rates based on ^{210}Pb were then used to calculate mass accumulation rates (MAR; g m^{-2} yr^{-1}) according to

$$\text{MAR (g cm}^{-2}\text{yr}^{-1}) = -1 * slope \text{ (g cm}^{-2}) * \text{decay constant } ^{210}\text{Pb (yr}^{-1}) \qquad (1)$$

$$\text{dry mass (g cm}^{-2}) = dw \text{ (g)} * \text{bulk density (g cm}^{-3}) * \frac{thickness \text{ (cm)}}{ww \text{ (g)}} \qquad (2)$$

Here the *slope* is the change of ln ^{210}Pb (Bq g^{-1}) as a function of cumulative dry mass (g cm^{-2}) and *dw* and *ww* refer to sediment
5   dry and wet weight, respectively. *Thickness* is the vertical thickness of each sampled sediment interval.

Modeling of OC burial and accumulation rates through time. The first-order decay of TOC was calculated using the power model of Middelburg (1989), which is a function of time (*t*), and an age-specific, empirically derived decay constant *k*:

$$\log k = -0.95 \log t - 0.81 \qquad (3)$$

Under the assumption of constant TOC accumulation (input) at the sediment surface, the Middelburg power model has proven
10   to be a good predictor of TOC content changes due to mineralization over time across diverse marine and lacustrine sediments (Burdige, 2007; Katsev and Crowe, 2015). Since lakes undergoing eutrophication are likely to experience changes in TOC accumulation and burial over time (Anderson et al., 2013; Anderson et al., 2014), and thus cannot be described by the power-model, we instead used the power model to provide an approximation for what TOC age profiles in sediment would be under the assumption that TOC accumulation had remained constant at today's values in the past. We then compare measured TOC
15   values (TOC$_{measured}$) in deeper layers to TOC predicted for these layers by the decay curve (TOC$_{modeled}$). Accordingly, subsurface TOC$_{measured}$ values that are higher (lower) than TOC$_{modeled}$ indicate higher (lower) TOC accumulation and burial rates than predicted by the power model. We calculate TOC burial rates according to

$$\text{TOC burial rate (g C m}^{-2}\text{yr}^{-1}) = \text{TOC}_{measured} \text{ (wt \%)} * \text{MAR (g m}^{-2}\text{yr}^{-1}) \qquad (4)$$

Assuming that changes in TOC accumulation rate, e.g. due to changes in water column primary productivity over time, are the main driver of differences between TOC$_{measured}$ and TOC$_{modeled}$, we use the decay function of the Power model – for each
20   sampled sediment horizon - reconstruct past TOC values (wt. %), for when this horizon was located at the sediment surface (TOC$_{reconstructed}$)

$$\text{TOC}_{reconstructed}(\text{wt. \%}) = \text{TOC}_{measured} \text{ (wt \%)} + \text{TOC loss (t)}(wt \%) \qquad (5)$$

Here 'TOC loss (t)' is the amount of TOC lost over time since the initial accumulation at the sediment surface. This was calculated based on the cumulative annual TOC loss predicted by k. We next reconstruct historic TOC accumulation rates for each sediment horizon when it was located at the sediment surface based on the following equation

$$TOC\ accumulation\ rates\ (g\ C\ m^{-2}yr^{-1}) = TOC_{reconstructed}\ (wt\ \%) * MAR\ (g\ cm^{-2}yr^{-1}) \qquad (6)$$

Modeling of respiration rates. In addition to examining eutrophication-related changes in organic carbon pool sizes over time, we investigated relationships between trophic state and total OC total respiration (mineralization) rates (RR_{total}). Here RR_{total} was defined as the sum of respiration rates to DIC (RR_{DIC}) and respiration rates to methane (methanogenesis) (RR_{CH4}), where RR_{DIC} and RR_{CH4} were modeled based on porewater concentration profiles of DIC and CH_4. DIC profiles were corrected for dissolution and precipitation of calcium carbonate using the Ca^{2+} porewater profiles (Fig. S5; measured during same run on IC as NH_4^+) (Hyun et al., 2017). Profiles of CH_4 and DIC were modelled using a power function with the formula

$$C_{cal}\ (mM) = C_0\ (mM) + a * z\ (cm)^{\ b} \qquad (7)$$

where C_{cal} is the calculated concentration of the model output, C_0 is the concentration of DIC at the sediment surface (0–1 cm) or of CH_4 in the shallowest sample of the methanogenesis zone, z is the depth in cm, and a and b are variables shaping the curve. The modeled concentrations where used to calculate a slope (mM cm^{-1}), which was calculated as follows:

$$slope\ (mM\ cm^{-1}) = a * b * z\ (cm)^{\ (b-1)} \qquad (8)$$

From this slope the *flux (f)* was calculated

$$f\ (mmol\ m^{-2}h^{-1}) = -slope\ (mM\ cm^{-1}) * D_{eff}\ (cm^2\ min^{-1}) * n \qquad (9)$$

where D_{eff} is the effective diffusion of DIC or CH_4 in water and where n is porosity. The effective diffusion at a specific temperature was corrected for the formation factor according to the formula:

$$D_{eff}\ (cm^2\ min^{-1}) = \frac{D\ (cm^2\ min^{-1})}{T^2} \qquad (10)$$

where D is the diffusion coefficient and T^2 is a factor calculated by multiplying porosity with the *formation factor (F)*. This formation factor was calculated using the formula:

$$F = 1.02 * (n^{-1.81}) \qquad (11)$$

where n is porosity, *1.02* is a unity factor (close to 1 means unity, i.e. same size and shape of particles) and 1.81 is an empirical factor. Based on a study in Lake Zug from Maerki et al. (2004), the unity factor was set to 1.02 and the empirical factor to 1.81. Diffusion coefficients (D_{eff}) as a function of temperature were calculated as D_{CH4} ($*10^{-5}$ cm^2 s^{-1}) = 0.0439 * T (C°) + 0.76 for CH$_4$ (Witherspoon and Saraf, 1965; Gruca-Rokosz, 2018), and as D_{HCO3-} ($*10^{-5}$ cm^2 s^{-1}) = 0.0002 * T^2 (C°) + 0.0172 T (C°) + 0.5463 for DIC (Zeebe, 2011).

The RR_{DIC} and RR_{CH4} were then calculated from the flux (mmol m^{-2} h^{-1}) for each depth interval (sediment depth z in cm) as follows:

$$RR_{DIC \text{ or } CH4}(\text{nmol C cm}^{-3}\,\text{h}^{-1}) \quad = \frac{(f_2 - f_1(\text{mmol } cm^{-2}\,h^{-1}))}{(z_2 - z_1\,(\text{cm}))} \qquad \textbf{\textit{(12)}}$$

In addition to determining RR_{total}, RR_{DIC}, and RR_{CH4}, we calculated the ratio of DIC to CH$_4$ production rates ($RR_{DIC}:RR_{CH4}$) as a proxy for the contribution of methanogenesis to total respiration by dividing RR_{DIC} with RR_{CH4} (dimensionless). Furthermore, we divided RR_{total} by the cell counts in each depth layer to estimate mean cell-specific respiration rates (RR_{cell}).

3 Results

In the first part of this section we document the impact of eutrophication, driven by water column P concentrations, on OC burial. In the second part we examine how these effects cascade further to alter respiration rates and distributions of respiration pathways in sediments.

3.1 Basic Sediment Parameters

An overview of the sedimentation rates, lamination intervals, bottom water temperatures, sediment porewater pH, and TOC content (TOC$_{measured}$) at each station is shown in Table 2. Average sedimentation rates (in cm yr^{-1}, ±standard deviation) in the eutrophic lakes (Lake Greifen: 0.32±0.04; Lake Zug: 0.28±0.08; Lake Baldegg: 0.29±0.03) are slightly higher than in mesotrophic Lake Zurich (0.23±0.03), and considerably higher than in oligotrophic Lake Lucerne: (0.13±0.06). Yearly laminations, indicating absence of significant macrofaunal sediment mixing, are present in several depth intervals at stations in Lake Greifen, Lake Baldegg, and Lake Zurich, but are absent from all stations in Lake Lucerne and Lake Zug (also see core photos in Fig. S3). These laminations mainly occur from the mid-upper to mid-bottom half of cores. The deep station of Lake Baldegg is an exception, in that laminations occur all the way to the bottom of the core. Bottom water temperatures at the time of sampling were between 5–9 °C. The pH in all sediment cores was close to neutral, and the average TOC contents were similar across all lakes, showing no relationship with trophic state.

3.2 Relationships between TOC and sediment depth

$TOC_{measured}$ in all five lakes ranges mostly from 2–4 % (total range: 1.1–5.3 %), with all stations showing a decrease with sediment depth (Fig. 2, Table 2). Despite this decrease, most lakes show local subsurface peaks between 10–30 cm depth, in particular the three eutrophic lakes. While TOC values between lakes show strong overlaps in the upper halves of cores, low TOC in deeper sediment layers suggests that historically two of the lakes, Lake Greifen and Lake Zug, were oligotrophic. This is confirmed by core images, which indicate that the deeper parts of the Lake Greifen and Lake Zug cores are dominated by organic-poor, calcium carbonate-rich clay ("Seekreide") (Fig. S3).

$TOC_{modeled}$ profiles, based on first-order decay of OC that was fitted to $TOC_{mesured}$ in surface sediments, compare to $TOC_{measured}$ as follows (Fig. 2): in the three eutrophic lakes, $TOC_{modeled}$ (locally) underestimates $TOC_{measured}$ in the top 10–30 cm, but matches or overestimates $TOC_{measured}$ data in lower parts of cores. In Lake Zurich, the model matches the measured data well, with only slight local underestimations of $TOC_{measured}$ in the upper halves of all three stations. In Lake Lucerne, the model generally matches $TOC_{measured}$ in the top ~15 cm, but consistently overestimates $TOC_{measured}$ in deeper layers.

Reconstructed past TOC accumulation rates at the sediment surface ($TOC_{reconstructed}$) suggest that sediment layers of the three eutrophic lakes that are at depths of 10–30 cm today in many cases received higher inputs of OC when they were located at the sediment surface than does today's sediment surface. By contrast, the $TOC_{reconstructed}$ data in Lake Zurich and Lake Lucerne do not indicate past periods of consistently higher TOC input to surface sediments than today. Irrespective of today's trophic state, the $TOC_{reconstructed}$ from all lake stations suggest that, on average, the TOC content at the sediment surface was lowest at the time that the deepest (and oldest) layers of sediment were deposited.

3.3 TOC burial and accumulation rates over time in relation to P concentrations

The correlation between trophic state and TOC burial becomes more clear when plotted against time (Fig. 3). Reflecting the higher sedimentation rates and similar $TOC_{measured}$ (Table 2), TOC burial rates increase with trophic state, being highest in the eutrophic Lake Baldegg and Lake Greifen and lowest in oligotrophic Lake Lucerne (Fig. 3). Reflecting the depth trends in TOC %, TOC burial rates overall decrease with sediment age but show distinct peaks in layers deposited from 1940–1990. The reconstructed TOC accumulation rates support this observation and suggest that peak TOC accumulation rates occurred between 1960–1980 in the eutrophic lakes. In addition, two stations in Lake Baldegg (21 and 45 m water depth) have a later peak in TOC accumulation rate that dates to the turn of the 21st century.

In Lake Greifen and Lake Zug increases in TOC burial and accumulation rate took place later than in Lake Baldegg, occurring mainly from 1920 onward, whereas in Lake Baldegg TOC burial and TOC accumulation rates were already increasing in the late 19th century. Incorporating changes in water column P concentrations from Fig. 1 into Fig. 3 shows that in the eutrophic Lake Greifen, Lake Baldegg, and Lake Zug increases in water column P concentrations occurred during the same time that TOC burial and accumulation rates increased during the 20th century. Peak P concentrations were measured between 1960 and 1980, when also the highest TOC accumulation rates were determined. Recent, strong decreases in water

column P concentrations match significant, albeit less marked decreases in TOC accumulation rates in Lake Greifen and Lake Zug. Comparing the time period of peak P concentrations to the time period from 2000-2014, P concentrations decrease by ~87 and 49% in Lake Greifen and Lake Zug, whereas average TOC accumulation rates only decrease by 24±11% and 22±5%, respectively. By contrast, in Lake Baldegg, where the decrease in P concentrations was the greatest during this time (~91%), there was no significant decrease in TOC accumulation rate (6±14%). In contrast to the eutrophic lakes, TOC accumulation rates in Lake Zurich and Lake Lucerne show no clear response to the (minor) temporary increases in water column P concentrations during the 20th century. Similarly, though P concentrations have decreased by ~75% (Lake Zurich) and ~89% (Lake Lucerne) between the time of the P concentration peak and 2000-2014, TOC accumulation rates have not changed significantly (Lake Zurich: 0±4%) or in fact increased, albeit insignificantly (Lake Lucerne: 11±17%).

Correlation analyses suggest that across all five lakes there is a highly significant ($p<0.001$), positive correlation between TOC accumulation rates and P concentrations (Fig. 4). For the entire time period from 1840–2016 considerable scatter and a low coefficient of determination ($R^2=0.28$) indicate that P concentrations only account for a minor portion of the observed variation in TOC accumulation rates (Fig. 4a). This changes, however, if only data from until the P peak are taken into account. Pairing these TOC accumulation rates with corresponding modeled and measured P concentrations (Fig. 4b) increases the R^2 to 0.54. When only TOC accumulation rates and measured P concentrations until the P peak are plotted (Fig. 4c), this R^2 increases further to 0.72. By contrast, the scatter increases ($R^2=0.23$), and the slope of the trendline decreases, when only TOC accumulation rates from after the P peak are correlated with measured P concentrations (Fig. 4a, d). Nonetheless, even during these recent decades, the correlation between TOC accumulation rates and P concentrations remains highly significant.

3.4 Distribution of microbial respiration reactions and microbial population size

Porewater and solid-phase concentrations of electron acceptors and end products of microbial respiration are presented in this section. These concentrations provide insights into the distributions and rates of different OC respiration reactions.

O_2. At all stations, O_2 concentrations decrease in a consistent, concave down-fashion, indicating high rates of O_2 consumption in the absence of significant O_2 production (Fig. 5, first row). Average O_2 penetration depths are lowest in Lake Baldegg and Lake Greifen (Table 3), indicating highest rates of aerobic respiration. Penetration depths increase with less eutrophic conditions in Lake Zug and Lake Zurich, and are greatest in Lake Lucerne, suggesting the lowest rates of aerobic respiration in the latter. Not surprisingly, the deep station from the hypoxic deep basin in Lake Zurich shows lower O_2 penetration than the shallower stations. In Lake Lucerne O_2 penetration increases from the shallow to the deep station. By contrast, the other three lakes show no trends related to water depth and are less variable in O_2 penetration depths.

NO_3^-. Bottom water concentrations of NO_3^- are higher in Lake Greifen (57–100 µM) and Lake Baldegg (93–103 µM) than in Lake Zurich (29–45 µM), Lake Lucerne (39–45 µM), or Lake Zug (21–25 µM) (Fig. 5, second row). The NO_3^- penetration

depths are lowest in Lake Greifen and Lake Baldegg. This combined with the high concentrations of nitrate indicate that denitrification rates are highest in these two eutrophic lakes. NO_3^- penetration depths increase in Lake Zurich, Lake Zug, and Lake Lucerne (Table 3). Combined with the water column NO_3^- concentrations this indicates that denitrification rates are next highest in Lake Zurich, followed by Lake Zug and Lake Lucerne. The wide ranges in bottom water NO_3^- concentrations in Lake Greifen and Lake Zurich, which have lower NO_3^- concentrations at the medium and deep station, and at the deep station compared to shallower stations, respectively, suggest water column denitrification in the (seasonally) hypoxic deeper parts of these lakes. Shallow and medium stations in Lake Greifen, Lake Zurich, and Lake Lucerne show have concave-up profiles in the top 1-2 cm of sediment, suggesting microbial NO_3^- production by nitrification in this layer.

Mn^{2+}. Dissolved Mn^{2+} was absent in significant concentrations in bottom water of all lakes, except the hypoxic deep station in Lake Zurich (35 µM), and the deepest stations in Lake Greifen (12 µM) and Lake Baldegg (6 µM) (Fig. 5, third row). At all stations, $[Mn^{2+}]$ increases in the upper sediment layers, suggesting microbial Mn(IV) reduction. Microbial Mn reduction occurs at lower rates than microbial Fe reduction, as indicated by lower $[Mn^{2+}]$ than $[Fe^{2+}]$, except in the deep station in Lake Zurich, where $[Mn^{2+}] > [Fe^{2+}]$ in the upper 30 cm. In all lakes except Lake Zug porewater $[Mn^{2+}]$ increases from shallow to deep stations, suggesting enhanced microbial Mn reduction rates from shallow to deep sediments. At most stations $[Mn^{2+}]$ increases in a concave-down fashion with depth, indicating continuous, albeit decreasing Mn^{2+}-reduction rates throughout the cores. Yet, reliable interpretations of the lower depth limit of Mn-reducing microbial activity are in some places confounded by local $[Mn^{2+}]$-peaks, by strong $[Mn^{2+}]$ decreases, and/or near-linear increases in $[Mn^{2+}]$ profiles in subsurface layers (deep stations in Lake Greifen, Lake Zurich, and Lake Lucerne, all stations in Lake Zug). Therefore, as indicated in Fig. 5 and Table 3, the lower depth limits of Mn-reduction are associated with considerable uncertainty.

Fe^{2+}. $[Fe^{2+}]$ is low (< 2 µM) or absent in bottom water and increases in porewater of surface sediment due to microbial Fe reduction (Fig. 5, fourth row). At all stations, the highest porewater $[Fe^{2+}]$ were present in the core bottoms, suggesting that the Fe reduction zone extends beyond the depth sampled (Table 3). In the eutrophic lakes, $[Fe^{2+}]$ accumulates rapidly, reaching 200–400 µM (Lake Baldegg), 60–100 µM (Lake Greifen), and 120–160 µM (Lake Zug) in the top 5 cm. Below, concentrations continue to increase, reaching 500–540 µM (Lake Baldegg), 250–500 µM (Lake Greifen), and 380–530 µM (Lake Zug) at the core bottoms. An exception is the deep station in Lake Baldegg, where the $[Fe^{2+}]$ has a local subsurface minimum at ~16 cmblf. Compared to the eutrophic lakes, Lake Zurich and Lake Lucerne appear to have lower microbial Fe-reducing activity, as evidenced by lower $[Fe^{2+}]$ concentration maxima (Lake Zurich: 95–310 µM; Lake Lucerne: 120–200 µM). Furthermore, Lake Zurich has divergent $[Fe^{2+}]$ profiles, having - within the upper 8cm - consistently low (< 4µM) concentrations (shallow and medium stations) or a near-linear concentration increase (deep station). Thus, porewater $[Fe^{2+}]$ profiles that clearly indicate Fe reduction are not established until depths >8 cm (also see 'Solid-phase Fe pools and EAC/EDC' in this section).

SO_4^{2-}. Bottom water concentrations of SO_4^{2-} differ significantly between lakes, but show no trend in relation to trophic state. The oligotrophic Lake Lucerne (150–170 µM), mesotrophic Lake Zurich (130–150 µM), and eutrophic Lake Greifen (130–140µM) have comparable concentrations, that clearly exceed those in the eutrophic Lake Baldegg (90–110 µM) and Lake Zug (48–53 µM) (Fig. 5, fourth row). At all stations, porewater [SO_4^{2-}] decreases steeply from the sediment surface downward, indicating significant microbial [SO_4^{2-}] reduction in surface sediment, but penetrates deeper than NO_3^-. SO_4^{2-} penetration depths are shallowest in the eutrophic Lake Greifen and Lake Baldegg and deepest in oligotrophic Lake Lucerne (Table 3).

CH_4. At all stations, [CH_4] increase with depth to the core bottom suggesting microbial methanogenesis beyond the cored intervals (Fig. 5, fifth row; Table 3). The highest [CH_4] are reached in sediments of Lakes Baldegg and Greifen (~8 and ~6 mM, respectively), and suggest higher methanogenesis rates than in sediments of the other lakes. Lake Zug reaches maximum [CH_4] of 2–4.5 mM at the core bottom. In Lake Zurich, the shallow and medium stations reach [CH_4] of 1.7 and 2.2 mM, respectively, whereas [CH_4] at the deep station reach 4 mM. In Lake Lucerne, [CH_4] remain < 1.5 mM, indicating the lowest methanogenesis rates among all five lakes. Strong increases in [CH_4] and δ^{13}C-DIC (*data not shown*) in the three eutrophic lakes and the deep station of Lake Zurich suggest that the methanogenesis zone already begins within the top 1 cm of sediment. By contrast, absence of significant [CH_4] accumulation and decreases in δ^{13}C-DIC (*data not shown*) indicate minimal methanogenesis, and instead significant rates of methane oxidation, in the top 2–3 cm of all Lake Lucerne stations and the shallow and medium stations in Lake Zurich.

Solid-phase bioavailable Fe pools and EAC/EDC. Bioavailable Fe(III) scatters between 0–5 mM in all lakes except in surface sediment of Lake Lucerne, where concentrations up to 25 mM were measured in a ~2 cm thick, oxidized surface layer (Fig. S6). Despite the absence of a clear decrease in bioavailable Fe(III), bioavailable Fe(II) increases with depth at all stations, from 5–10 mM at the surface to 30–50 mM in deeper layers, consistent with microbial reduction of Fe(III), that is apparently not limited to the 'bioavailable' fraction, to the bottom of all cores (Fig. S6). The steepest increase in Fe(II) typically occurs in the top ~5cm, suggesting that iron reduction rates are highest in surface sediments. The electrochemical measurements confirm the trends in bioavailable Fe(II) and Fe(III), with a greater EDC than EAC everywhere except in the oxidized surface layer of Lake Lucerne, strong scatter in the EAC throughout all cores, and a general increase in EDC with depth (Fig. S6).

3.5 Total and cell-specific microbial respiration activity

At all stations, DIC concentrations increase with depth in a typical concave-down fashion that indicates highest rates of total respiration in surface sediments, and a decrease in microbial respiration rates with depth (Fig. 6, first column).

Sediments from Lake Baldegg and Lake Greifen show the highest DIC concentrations, reaching 6–9 mM near the core bottom. With a decrease in trophic state, there is a decrease in DIC accumulation, indicative of lower rates of microbial respiration. Accordingly, DIC maximum concentrations in the core bottoms reach 5–6 mM in Lake Zug, 4–5 mM in Lake

Zurich, and 3–4 mM in Lake Lucerne. Similar trends in relation to trophic state are present for NH_4^+ concentrations, which are a proxy for the microbial breakdown of N-containing organic matter, such as amino acids and nucleic acids (Fig. S5).

Consistent with the DIC profiles, the modeled RR_{total} decrease with depth in all 5 lakes (Fig. 6, second column). While RR_{total} decreases by approximately two orders of magnitude in all lakes, sediment horizons from eutrophic lakes have higher
5 average RR_{total} than the same sediment depths in oligotrophic lakes. For instance, the mean RR_{total} in the shallowest layers is 2.1 nmol C cm^{-3} h^{-1}, 5.8 nmol C cm^{-3} h^{-1}, and 1.6 nmol C cm^{-3} h^{-1} in Lake Greifen, Lake Baldegg, and Lake Zug, respectively, compared to ~1 nmol C cm^{-3} h^{-1} in both Lake Zurich and Lucerne. This difference is maintained all the way to the bottom of the cores, where values in Lake Greifen (0.05 nmol cm^{-3} h^{-1}), Lake Baldegg (0.03 nmol cm^{-3} h^{-1}), and Lake Zug (0.02 nmol cm^{-3} h^{-1}) remain higher than in Lake Zurich and Lake Lucerne (both 0.01 cm^{-3} h^{-1}).

10 The ratio of RR_{DIC}:RR_{CH4} indicates a higher contribution of methanogenesis to RR_{total} throughout the sediment cores of the three eutrophic lakes (Fig. 6, third column). This difference is most pronounced in surface sediments where mean RR_{DIC}:RR_{CH4} values are 0.3 in Lake Greifen, 1.2 in Lake Baldegg, and 2.3 in Lake Zug, compared to 3.5 in Lake Zurich and 12 in Lake Lucerne. With increasing sediment depth, the mean RR_{DIC}:RR_{CH4} become more similar between the lakes. While the RR_{DIC}:RR_{CH4} remains fairly stable with depth in Lake Greifen, all other lakes display a decrease in RR_{DIC}:$RR_{CH4}$with depth,
15 indicating a depth-dependent increase in the contribution of methanogenesis to total respiration.

In all five, lakes, microbial cell numbers decrease with depth. Cell counts in surface sediments range from 10^9–10^{10} cm^{-3} and decrease to ~10^7–10^9 cm^{-3} in deeper layers (Fig. 6, forth column). Cell numbers do not reflect trophic state or RR_{total}. On the contrary, though there are strong overlaps between the lakes, the highest average cell counts in surface sediments are from mesotrophic Lake Zurich and oligotrophic Lake Lucerne, and the highest average cell counts in deeper layers are from
20 Lake Zurich (Fig. S7). No clear subsurface peaks in cell counts, e.g. as relic signals of periods of peak eutrophication or TOC accumulation, are evident either. Instead cell numbers show considerable scatter between stations (especially Lake Baldegg and Lake Zurich) and abrupt changes between adjacent sediment intervals (especially Lake Greifen, Lake Baldegg, and the deep station in Lake Zurich). The abrupt drop in cell concentrations in the lower half of the core from the deep station in Lake Zurich matches a lithological shift toward organic-poor, carbonate clay ("Seekreide") layers, which are turbidites from upslope
25 of the lake (Fig. S3). By comparison, the fluctuations in cell counts in Lake Baldegg and Lake Greifen do not match any measured geochemical or sedimentological parameters.

Reflecting the high variability in cell counts, the RR_{cell} are also highly variable. Nonetheless, there are several clear trends. RR_{cell} are highest at the sediment surface and then decrease, stabilizing within the top 5–10 cm, and showing only minor changes throughout the remainder of the cores. Though the mean RR_{cell} of surface sediment is not a good predictor of trophic
30 state, with Lake Zurich having the highest RR_{cell} (0.41 pmol C cell^{-1} yr^{-1}), the RR_{cell} reflect trophic state below 5–10 cm depth (Lake Greifen: ~0.005 pmol C cell^{-1} yr^{-1}; Lake Baldegg: ~0.01 pmol C cell^{-1} yr^{-1}; Lake Zug: ~0.004 pmol C cell^{-1} yr^{-1}; Lake Zurich: ~0.002 pmol C cell^{-1} yr^{-1}; Lake Lucerne: ~0.0009 pmol C cell^{-1} yr^{-1}). Based on a Paired Samples Wilcoxon Test, the average RR_{cell} are not significantly different between Lake Baldegg and Lake Greifen, but are significantly different between Lake Baldegg and Lake Zug (p=0.04), Lake Zug and Lake Zurich (p=0.003), and Lake Zurich and Lake Lucerne (p=0.02).

3.6 *Relationships of RR$_{total}$, cell counts, and RR$_{cell}$ with sediment age*

Due to differences in sedimentation rates between and within the lakes, analyzing RR$_{total}$, microbial population size, and RR$_{cell}$ in the context of sediment depth alone does not provide reliable insights into the impacts of eutrophication. We therefore subdivided the study period into 6 time intervals, the pre-eutrophication era (1840–1900), three intervals of the eutrophication era (early: 1900–1940, mid: 1940–1960, peak: 1960–1980), and two intervals of the "post-eutrophication" era (1980–2000, 2000–2016). Within each time interval, we averaged the data from each station (Fig. 7). Due to the high intra-lake and intra-core variability, the standard deviations are high and in many cases overlap. Nonetheless, several insights into the relationships between eutrophication, microbial population size, and microbial respiration rates can be gained.

In all lakes, RR$_{total}$ decreases with sediment age in a near-asymptotic way, with a one order of magnitude decrease across sediment intervals from the last ~60 years, followed by minor decreases in older layers (Fig. 7a). Thus, sediments deposited during the pre-eutrophication, early and mid-eutrophication periods (i.e. from 1840-1960) have similar RR$_{total}$ today, even though TOC accumulation rates changed significantly across these periods (Fig. 3).

Cell numbers decrease with sediment age (Fig. 7b). Furthermore, the earlier observation (Fig. 6) that eutrophic lakes do not have higher cell counts than oligotrophic lakes is confirmed. When plotted against age since 1900, Lake Lucerne and Lake Zurich even have consistently higher average cell numbers than the eutrophic lakes. Depth-related decreases in cell numbers are also different between the lakes. The two lakes that went from highly oligotrophic to eutrophic (Lake Greifen, Lake Zug) have ~20fold (Lake Greifen) and ~30fold (Lake Zug) decreases in average cell numbers from 2000–2016 to 1840–1900. By comparison, cell counts in the other three lakes have smaller changes in cell numbers with sediment age (Lake Baldegg: ~4fold; Lake Zurich: ~8fold; Lake Lucerne: ~6fold).

The RR$_{cell}$ decrease within the first ~4 decades since deposition, but stabilize in sediments that were deposited before 1980 (Fig. 7c). The only exception is Lake Baldegg, where the RR$_{cell}$ remains stable throughout all layers deposited since 1940, and only decreases in horizons deposited prior to 1940. The decrease in RR$_{cell}$ over time since deposition is approximately one order of magnitude in Lakes Greifen, Baldegg, Zug, and Lucerne, and two orders of magnitude in Lake Zurich.

4 Discussion

Our results show that eutrophication of lakes in central Switzerland, driven by anthropogenic input of P, has had a strong impact not only on lake water columns but also on sediments. While the average TOC content is not a good indicator of trophic state (Table 2), changes in TOC$_{reconstructed}$ with depth indicate a significant impact of eutrophication on the sedimentary TOC sink (Fig. 2) with significant increases in TOC burial and accumulation rates over the last century (Fig. 3). Correlations between TOC accumulation rates and water column P concentrations through time (Fig. 3) suggest that lakes with the highest increases in P concentrations also had the highest increases in TOC accumulation (and burial) rates in their sediments. The relationship between P concentrations and TOC accumulation rates was strongest during the period of rapid P concentration increase in the mid 20th century (Fig. 4). Yet, even though water column P concentrations in most lakes have decreased close to pre-

eutrophication levels since the ~1970s, TOC burial and accumulation rates in eutrophic lakes remain significantly higher than before the eutrophication era (Figs. 3 and 4).

Despite the increase in TOC burial, lake sediments are not a static sink for OC. Increases in TOC accumulation and burial increase mineralization by stimulating microbial respiration (Fig. 6). Water column-derived electron acceptors, such as O_2 and nitrate, are depleted at shallower depths in eutrophic lakes compared to lakes with a lower trophic status (Fig. 5; Table 3). Similarly, the contribution of methanogenesis to total respiration is greater (Fig. 6), and significant rates of methanogenesis occur at shallower sediment depths in the eutrophic lakes (Fig. 5, Table 3). These eutrophication-related changes in respiration rates are, however, not reflected in the vertical zonation of microbial respiration pathways with respect to each other. Instead, the depth intervals of denitrification, Mn(IV) reduction, Fe(III) reduction, sulfate reduction, and methanogenesis show strong overlaps, independent of lake trophic state (Fig. 5; Table 3). Also, although higher TOC input and respiration rates appear to increase cell-specific respiration rates, they do not result in a higher microbial population size (Fig. 6). Instead, the lakes that were least affected by eutrophication (Lake Zurich, Lake Lucerne) have the highest cell counts in sediments deposited during the period of peak eutrophication from 1940–2000 (Fig. 7).

In the following sections, we discuss in detail the *(i)* response of TOC accumulation and burial to eutrophication, *(ii)* potential effects of eutrophication mitigation measures on TOC burial and accumulation, *(iii)* the relationship between zonation and rates of dominant respiration processes and trophic state, and *(iv)* the relationship between total respiration rates, microbial population size, and trophic state.

(i)   Response of TOC burial to eutrophication

The TOC burial rates in this study match estimates from previous studies. The average annual burial rate of 27 g C m^{-2} yr^{-1} for sediments deposited from 1960 to 1990 at the deep station of Lake Baldegg is only slightly lower than the estimate of Teranes and Bernasconi (2000) (~30 g C m^{-2} yr^{-1}) for the same location and time interval. A recent study on Lake Baldegg determined average OC burial rates of 32.3 g C m^{-2} yr^{-1} for the top 2–10 cm of stations from water depths of 23, 40, 64 m (Steinsberger et al., 2017), which are very similar to the 34 g C m^{-2} yr^{-1} for the top 2–10 cm of our three 3 stations. The average TOC burial rates from our study (13.8 to 33.3 g C m^{-2} yr^{-1} from 1840 to 2016), moreover, fall within the range of 116 lakes from different ecoregions in Minnesota (3 to 184 g C m^{-2} yr^{-1} from 1800–2010) (Anderson et al., 2013), and from 93 lakes in 11 countries across Europe (Anderson et al., 2014). The latter study, estimated that average burial rates increased on average 2.5-fold from 17 g C m^{-2} yr^{-1} in the 19th century to 40 g C m^{-2} yr^{-1} in 1900–1950, and again 1.5-fold to 60 g C m^{-2} yr^{-1} after 1950 (Anderson et al., 2014). By comparison, we estimate a smaller impact on TOC burial in the 5 lakes studied. Our average±SD burial rates (in g C m^{-2} yr^{-1}) of 14±6 (1900–1940), 17±6 (1840–1900), 22±8 (1940–1960), 27±10 (1960–1980), 27±9 (1980–2000), and 29±8 (2000–2016) only correspond to a doubling in average TOC burial rates from the 19th century to after 1960. Incorporating estimates of TOC loss over time does not change these interpretations. According to the Middelburg power model (Middelburg, 1989), the biggest TOC loss occurs in year 1 after deposition (~16%), followed by ~2% over the following 15 years (in our

case 2000–2015), ~1% over the following 20 years (1980–2000), and ~1.5% over the following 140 years (1840–1980). Our burial rates and those determined in the other above studies were all determined on sediments that were over 1 year old.

While our data indicate that TOC burial and accumulation rates increase with eutrophic conditions, it is important to distinguish between natural background TOC accumulation rates, and increases in TOC accumulation rates above these background rates due to eutrophication. For instance, we estimate that in Lake Greifen and Lake Baldegg TOC accumulation rates were already 2–3 times higher than in Lake Lucerne before the period of eutrophication (Fig. 3). Lake Zug and Lake Zurich also had higher average TOC accumulation rates than Lake Lucerne prior to eutrophication. Presumably variables besides eutrophication, e.g. natural OM inputs from the watershed or surrounding riparian vegetation, and physical factors, e.g. sediment focusing, lake area, water depth, and water residence times, contribute to these natural differences between the five lakes. While we do not have data on OM contributions from land or riparian zones, physical factors may indeed (partially) drive the natural differences in TOC accumulation rates between the five lakes (Fig. S8 and Table S1). In line with previous studies (Dean and Gorham, 1998; Heathcote and Downing, 2012), we observe a strong negative linear relationship between lake area and TOC accumulation rate (Fig. S8a; R^2=0.99). This may be (partially) due to dilution effects, as lake volume also shows a strong negative linear relationship with TOC accumulation rates (Fig. S8b; R^2=0.91). By contrast, water residence time shows no correlation with TOC accumulation rates (Fig. S8c). Other variables that often drive the distribution of TOC accumulation within lakes, e.g. water depth and sediment focusing (Lehman, 1975; Davis and Ford, 1982; Blais and Kalff, 1995), show no clear trends in relation to TOC accumulation rates (Fig. S8d–e) and SI Text 2.

In spite of pre-existing differences in lake-specific TOC accumulation rates, the clear changes in TOC accumulation (and burial) rates over time, which correlate with water column P concentrations and coincide with anoxic events and algal blooms (Figs. 1, 3, and 4), indicate a strong impact of eutrophication. Similar increases in OC burial and accumulation in lake sediments due to eutrophication have been reported elsewhere (Gorham et al., 1974; Dean and Gorham, 1998; Heathcote and Downing, 2012). A combination of variables may drive this eutrophication-related increase in OC burial. First, the increase in primary production due to lake P fertilization promotes water column biomass production, and increases biomass deposition to the lake floor. Increased OM loading then stimulates aerobic OM catabolism, which causes water column anoxia, and further promotes OM preservation and burial (Lehmann et al., 2002; Sobek et al., 2009; Katsev and Crowe, 2015).

(ii)   *Effects of eutrophication mitigation measures on TOC burial*

Since the period of peak eutrophication, water column P concentrations have decreased back to pre-eutrophication levels, mainly as a result of wastewater treatment combined with P precipitation systems and removal of phosphate from detergents (Fig. 1, SI Text 1). This has coincided with significant decreases in TOC accumulation rates in Lake Greifen (24±11%) and Lake Zug (22±5%), but not in Lake Baldegg (6±14%; *discussed later in this section*). Presumably, the decreases in Lake Greifen and Lake Zug were mainly driven by reduced primary production. Decreased TOC preservation due to increased O_2

exposure time was probably less important, since seasonal water column anoxia continued for decades after the decrease in TOC accumulation rates in Lake Greifen and Lake Zug (Figs. 1 and 3; BAFU, 2013; AquaPlus, 2001; AquaPlus 2004).

Despite the observed decreases in TOC accumulations in two of the three eutrophic lakes, our calculated TOC accumulation rates for the period after peak eutrophication have remained well above those during pre-eutrophication times (Fig. 3). Furthermore, the correlation between P concentrations and TOC accumulation rates has become weaker since the decrease in P concentrations (Fig. 4b–d). A potential reason for the reduced coupling between P concentrations and TOC accumulation rates is remobilization of P, which accumulated in sediments during periods of high P inputs, into overlying water (Rippey and Anderson, 1996; Boyle, 2001; Meals et al., 2010; Giles et al., 2016). Remobilization of P from sediments can sustain high primary productivity and lower water quality for years to decades after substantial decreases in P inputs (Lotter, 2001; Giles et al., 2016). Such remobilization of P is not necessarily evident based on total P concentrations as most remobilized P is present in highly bioavailable inorganic form. By contrast, most P from wastewater or manure is present in organic form and has to be mineralized to inorganic P by microbial organotrophs to become available to primary producers. Slower turnover of organic P from wastewater and runoff may partially explain why P concentrations soared during the period of peak eutrophication, but are low today, despite a significant release of remobilized P from sediments.

Our data, furthermore, indicate that artificial mixing does not substantially reduce TOC accumulation and burial, and in fact might counteract reductions in TOC accumulation and burial caused by reduced P inputs. In Lake Baldegg, artificial aeration and oxygenation were implemented in 1982/3 (Stadelmann and Escher, 2002) and have eliminated bottom water anoxia, thereby increasing O_2 exposure time of most detrital OC from hours, during sinking through the water column (Bloesch and Burns, 1980; Lehmann et al., 2002), by an additional 3–4 months within oxic sediment [notes: (1) O_2 exposure time in sediment was estimated by dividing O_2 penetration depth by sedimentation rate; (2) there was no strong bioturbation in surface sediment, as chironomid larvae were absent and deposit-feeding oligochaetes were mainly observed at depths > 5 cmblf]. Nonetheless, TOC accumulation and burial rates have not decreased significantly since then, confirming initial observations made by Gächter and Wehrli (1998) after 10 years of artificial aeration. Given that Lake Greifen and Lake Zug, which were not artificially mixed, had significant reductions in TOC accumulation rates, we speculate that water column mixing may even indirectly promote high TOC burial rates in Lake Baldegg. Accordingly, mixing creates an "artificial upwelling" that efficiently transports remobilized P, which has diffused from sediments into bottom water, to the photic zone. In the photic zone, this P is turned over rapidly and sustains high growth rates of photosynthetic organisms. High rates of primary production then sustain the continually high rates of TOC accumulation and burial in lake sediments. If this interpretation is correct, then we would predict TOC burial and accumulation rates in Lake Greifen to remain stable or increase since the beginning of artificial mixing in 2009. Comparing TOC accumulation rate data from 2000-2009 to data from 2010-2014 suggests this could be the case, as TOC accumulation rates have increased, albeit variably, at all three stations since then by on average 6±5%.

(iii)   ***Zonation and rates of dominant respiration processes***

The vertical distribution of dominant respiration reactions in the five lakes generally matches what would be expected based on differences in total respiration rates. Electron acceptors that diffuse from bottom water into sediment (O_2, nitrate, sulfate) are depleted at shallower depths in eutrophic than in the meso- and oligotrophic lakes due to higher respiration rates fueled by higher TOC input. Less reactive solid-phase electron acceptors (Mn(IV), Fe(III)), and electron acceptors that are produced at high rates within sediments (CO_2), extend deeper into cores, and even throughout cores in the case of Fe(III) and CO_2. While Mn reduction rates appear to be mainly controlled by Mn supply, which is driven by geochemical focusing (Engstrom and Wright Jr, 1984; Schaller and Wehrli, 1996; Naeher et al., 2013), both Fe reduction and methanogenesis rates increase with trophic state, most likely as a result of increased electron donor and acceptor supply from the enhanced breakdown of OM.

In addition to this general effect of eutrophication on microbial respiration rates, a clear vertical separation of respiration reactions involving different electron acceptors is absent, independent of trophic state (Fig. 5). One possible reason is that electron donor concentrations are not under thermodynamic control (Hoehler et al., 1998), and that free energy yields of all respiration reactions are above previously observed minimum thresholds per reaction (10 to 20 kJ mol^{-1}; Hoehler et al. (2001)). This could potentially indicate that respiration reactions in sediments were not in steady-state at the time of sampling, e.g. due to temperature changes, redox fluctuations, mortality, and/or bioturbation (Hoehler et al., 1999; Lever and Teske, 2015; Chen et al., 2017). Chemical microenvironments with divergent redox conditions may also enable different respiration reactions to occur physically separated but in close proximity to each other (Anderson and Meadows, 1978; Canfield, 1989; Oda et al., 2008). "Non-competitive" substrates, such as the C1 compounds methanol, dimethylsulfide, and trimethylamine, which are consumed by some methanogens and not by most sulfate reducers, and enable coexistence of these methanogens with sulfate reducers in sulfate reducing marine sediment (Oremland and Polcin, 1982; Xiao et al., 2017) are also possible. However, previous research on lake sediments indicates that non-competitive substrates only support a small fraction of total methanogenesis (Conrad et al., 2011; Liu et al., 2017). Moreover, research on the five lakes studied here suggests dominance of H_2/CO_2-consuming *Methanomicrobiales*, and that methanogenesis from H_2/CO_2 is thermodynamically not favorable in most methanogenic horizons (Michel & Lever, *unpubl. data*). Thus, as a working hypothesis, microenvironments with divergent redox conditions might explain the strong spatial overlaps in respiration reactions.

(iv)   *Respiration rates and total microbial population size*

Total respiration rates (RR_{total}) decrease with sediment depth at all stations, indicating an increase in the OM degradation state over time, as microorganisms selectively mineralize the more reactive OM pools. The higher RR_{total} in eutrophic compared to meso- and oligotrophic lakes, even in buried intervals that were deposited around the same time, suggests that the eutrophication-related stimulation of RR_{total} persists over many decades, possibly due to the higher amounts of TOC (both reactive and non-reactive) that were initially deposited. Despite this continued OM mineralization, only a small fraction of originally accumulated TOC is mineralized in these older layers (also see final paragraph of Discussion section (i)).

Overall cell numbers in the range of 10^8 to 10^{10} cells cm^{-3} (Fig. 6 and S7) are in a similar range as other lake sediments (Bostrom et al., 1989; Haglund et al., 2003; Schwarz et al., 2007). Surprisingly, despite the higher TOC burial and RR_{total}, the three eutrophic lakes have lower average cell numbers than Lake Zurich and Lake Lucerne (Fig. 6 and S7). Possibly, the shallower depletion of O_2, nitrate, sulfate, and Mn(IV) in eutrophic lakes causes a larger fraction of respiring microorganisms to depend on energetically less favorable methanogenesis. Thus, cells in eutrophic lake sediment would have less energy available per cell despite having more available electron donors and higher RR_{cell}. Though possible, this scenario is unlikely given that the vast majority of anaerobic microorganisms in sediment are probably involved in fermentation reactions (Lever, 2013), and that methanogens account for at most a few percent of the microbial populations in cores from this study (Michel & Lever, *unpubl. data*). Alternative explanations for the lower cell counts in eutrophic lakes might be higher toxic contaminant loads (Pritchard and Bourquin, 1984), higher viral mortality (Fischer and Velimirov, 2002), or enhanced predation by oligochaete worms. The latter were highly abundant to sediment depths of > 20cm in the eutrophic lakes (Fiskal et al., *unpubl.*).

5   Conclusions

Based on sedimentary records from five lakes differing in eutrophication history over the last ~180 years, we demonstrate clear links between human activity on land, water column eutrophication, and OC burial in lake sediment. By combining high resolution historic data on water column P concentrations with reconstructed past TOC accumulation rates, we show that anthropogenic input of P to lake ecosystems, most likely by increasing water column primary production and TOC sedimentation, is a key driver of TOC input to and TOC burial within lake sediment. This relationship between P concentrations in the water and TOC accumulation and burial rates in sediments was strongest during the period leading to the eutrophication peak in the 1970s. Since then, despite reductions in P concentrations by 50-90% across all five lakes, TOC accumulation rates have decreased by ~20-25% in two of the eutrophic lakes (Lake Greifen, Lake Zug), and not significantly in the other three lakes, the eutrophic Lake Baldegg, the mesotrophic Lake Zurich, and the oligotrophic Lake Lucerne. This relatively small or absent decrease in TOC accumulation rates is potentially due to the efficient remobilization of sedimentary P by microbial diagenesis and water column mixing. The fact that the highly eutrophic Lake Baldegg, which has been artificially mixed and aerated for >35 years to mitigate water column anoxia, shows no significant decrease in TOC accumulation rates or TOC burial, indicates that water column mixing and aeration is not effective at reducing P release from sediment or at controlling water column primary productivity, but might even have the opposite effect by rapidly transferring this P to the photic zone.

In addition to documenting the effects of eutrophication on TOC accumulation and burial, we investigate effects of eutrophication on microbial TOC mineralization processes and microbial population size. We show that eutrophic lakes have higher respiration rates (total and cell-specific), and a higher contribution of methanogenesis to total respiration, than lakes with a lower trophic status. Yet, trophic state does not affect the zonation of microbial respiration reactions. Instead, independent of trophic state, low-energy reactions, such as methanogenesis, occur well into sediment layers with

denitrification, manganese reduction, and even aerobic respiration, possibly due to the presence of geochemically distinct microenvironments. Despite the higher respiration rates in the eutrophic lakes, we observe equal or even lower cell abundances in eutrophic compared to mesotrophic and oligotrophic lake sediment. This indicates that, for yet unknown reasons, electron donor supply and/or microbial energy availability is decoupled from microbial biomass in sediments of these five lakes.

Data availability

The data used in this manuscript will be made available on PANGAEA after the manuscript is published.

10 **Author contribution**

A.F., L.D., X.H., A.M., P.E., L.L., R.Z., N.D. and M.A.L. helped with sample collection, and/or measurements. A.F., N.D., M.H.S., S.B., M.S. and M.A.L substantially contributed to the interpretation of data. A.F. and M.A.L. wrote the manuscript. M.A.L. designed the study and acquired the funding for the project. All authors commented on the manuscript and approved the final version of the manuscript.

Conflict of interest

The authors declare no conflict of interests.

Acknowledgements

20 We thank Madalina Jaggi for sample preparation and measurements. Special thanks to Adrian Gilli (ETHZ) and all technicians, especially Irene Brunner, Alfred Lück and Alois Zwyssig from EAWAG for great help with sampling and downstream analysis. Many thanks to Iso Christl, Rachele Ossola, Joep van Dijk and Andreas Brand for consulting regarding measurement and analyses. We thank Meret Aeppli and Nicolas Walpen for the introduction to electrochemical analyses. We thank Joachim Hürlimann for kindly providing reconstructed phosphorus data from Lake Greifen and Lake Zug and Andre Lotter for 25 providing reconstructed phosphorus data for Lake Baldegg and Lake Lucerne. This project is funded by the Swiss National Science Foundation (project 205321_163371: "Role of bioturbation in controlling microbial community composition and biogeochemical cycles in marine and lacustrine sediments" awarded to Mark A. Lever).

References

Anderson, J. G. and Meadows, P. S.: Microenvironments in Marine-Sediments, P Roy Soc Edinb B, 76, 1-16, 1978.

Anderson, N. J., Bennion, H., and Lotter, A. F.: Lake eutrophication and its implications for organic carbon sequestration in Europe, Global Change Biology, 20, 2741-2751, 2014.

5 Anderson, N. J., Dietz, R. D., and Engstrom, D. R.: Land-use change, not climate, controls organic carbon burial in lakes, P Roy Soc B-Biol Sci, 280, 2013.

AquaPlus 2001: Entwicklung des Gesamtphosphors im Zugersee anhand der im Sediment eingelagerten Kieselalgen. Bericht zuhanden des Amtes für Umweltschutz des Kantons Zug, 48 S.

AquaPlus 2004: Untersuchung der Fliessgewässer und Seen im Kanton Zug und im Einzugsgebiet des Zugersees. Bericht zuhanden des
10 Amtes für Umweltschutz des Kantons Zug, 86 S.

AquaPlus 2004: Entwicklung des Gesamtphosphors im Greifensee anhand der im Sediment eingelagerten Kieselalgen. Bericht zuhanden des Amtes für Abfall, Wasser, Energie und Luft des Kantons Zürich.

BAFU,   2013:   Einzugsgebietsgliederung   Schweiz   EZGG-CH,   Bundesamt   für   Umwelt,   Bern. http://www.bafu.admin.ch/hydrologie/01835/11452/index.html., last access: 18 March 2019.

15 Bastviken, D., Cole, J., Pace, M., and Tranvik, L.: Methane emissions from lakes: Dependence of lake characteristics, two regional assessments, and a global estimate, Global Biogeochem Cy, 18, 2004.

Battin, T. J., Luyssaert, S., Kaplan, L. A., Aufdenkampe, A. K., Richter, A., and Tranvik, L. J.: The boundless carbon cycle, Nat Geosci, 2, 598-600, 2009.

Binford, M. W.: Calculation and uncertainty analysis of 210Pb dates for PIRLA project lake sediment cores, Journal of Paleolimnology, 3,
20 253-267, 1990.

Blais, J. M. and Kalff, J.: The Influence of Lake Morphometry on Sediment Focusing, Limnol Oceanogr, 40, 582-588, 1995.

Bloesch, J. and Burns, N. M.: A Critical-Review of Sedimentation Trap Technique, Schweiz Z Hydrol, 42, 15-55, 1980.

Bostrom, B., Pettersson, A. K., and Ahlgren, I.: Seasonal Dynamics of a Cyanobacteria-Dominated Microbial Community in Surface Sediments of a Shallow, Eutrophic Lake, Aquat Sci, 51, 153-178, 1989.

25 Boyle, J.: Redox remobilization and the heavy metal record in lake sediments: a modelling approach, Journal of Paleolimnology, 26, 423-431, 2001.

Braunschweig, J., Bosch, J., Heister, K., Kuebeck, C., and Meckenstock, R. U.: Reevaluation of colorimetric iron determination methods commonly used in geomicrobiology, J Microbiol Meth, 89, 41-48, 2012.

Breitburg, D.: Effects of hypoxia, and the balance between hypoxia and enrichment, on coastal fishes and fisheries, Estuaries, 25, 767-781,
30 2002.

Buergi, H. R. and Stadelmann, P.: Change of phytoplankton diversity during long-term restoration of Lake Baldegg (Switzerland), Int Ver Theor Angew, 27, 574-581, 2000.

Burdige, D. J.: Preservation of organic matter in marine sediments: Controls, mechanisms, and an imbalance in sediment organic carbon budgets?, Chem Rev, 107, 467-485, 2007.

35 Canfield, D. E.: Reactive Iron in Marine-Sediments, Geochim Cosmochim Ac, 53, 619-632, 1989.

Canfield, D. E., Kristensen, E., and Thamdrup, B.: Aquatic Geomicrobiology, Adv Mar Biol, 48, 1-640, 2005.

Canfield, D. E. and Thamdrup, B.: Towards a consistent classification scheme for geochemical environments, or, why we wish the term 'suboxic' would go away, Geobiology, 7, 385-392, 2009.

Capone, D. G. and Kiene, R. P.: Comparison of Microbial Dynamics in Marine and Fresh-Water Sediments - Contrasts in Anaerobic Carbon
40 Catabolism, Limnol Oceanogr, 33, 725-749, 1988.

Chen, X. H., Andersen, T. J., Morono, Y., Inagaki, F., Jorgensen, B. B., and Lever, M. A.: Bioturbation as a key driver behind the dominance of Bacteria over Archaea in near-surface sediment, Sci Rep-Uk, 7, 2017.

Cline, J. D.: Spectrophotometric Determination of Hydrogen Sulfide in Natural Waters, Limnol Oceanogr, 14, 454-&, 1969.

Cole, J. J., Prairie, Y. T., Caraco, N. F., McDowell, W. H., Tranvik, L. J., Striegl, R. G., Duarte, C. M., Kortelainen, P., Downing, J. A.,
45 Middelburg, J. J., and Melack, J.: Plumbing the global carbon cycle: Integrating inland waters into the terrestrial carbon budget, Ecosystems, 10, 171-184, 2007.

Conley, D. J., Paerl, H. W., Howarth, R. W., Boesch, D. F., Seitzinger, S. P., Havens, K. E., Lancelot, C., and Likens, G. E.: ECOLOGY Controlling Eutrophication: Nitrogen and Phosphorus, Science, 323, 1014-1015, 2009.

Conrad, R., Noll, M., Claus, P., Klose, M., Bastos, W. R., and Enrich-Prast, A.: Stable carbon isotope discrimination and microbiology of
50 methane formation in tropical anoxic lake sediments, Biogeosciences, 8, 795-814, 2011.

Correll, D. L.: Phosphorus: A rate limiting nutrient in surface waters, Poultry Sci, 78, 674-682, 1999.

Cubasch, U., Wuebbles, D., Chen, D. L., Facchini, M. C., Frame, D., Mahowald, N., Winther, J. G., Brauer, A., Gates, L., Janssen, E., Kaspar, F., Korper, J., Masson-Delmotte, V., Meinshausen, M., Menne, M., Richter, C., Schulz, M., Schulzweida, U., Stevens, B., Sutton, R., Trenberth, K., Turkes, M., and Ward, D. S.: Climate Change 2013 The Physical Science Basis Working Group I Contribution to the Fifth

Assessment Report of the Intergovernmental Panel on Climate Change Introduction, Climate Change 2013: The Physical Science Basis, 2014. 119-158, 2014.

Davis, M. B. and Ford, M. S. J.: Sediment Focusing in Mirror Lake, New-Hampshire, Limnol Oceanogr, 27, 137-150, 1982.

Dean, W. E. and Gorham, E.: Magnitude and significance of carbon burial in lakes, reservoirs, and peatlands, Geology, 26, 535-538, 1998.

5   Deng, L., Fiskal, A., Han, X., Dubois, N., Bernasconi, S. M., and Lever, M. A.: Improving the accuracy of flow cytometric quantification of microbial populations in sediments: importance of cell staining procedures, Front Microbiol, 10, 720, 2019.

Drake, H. L., Kusel, K., and Matthies, C.: Acetogenic Prokaryotes, Prokaryotes: A Handbook on the Biology of Bacteria, Vol 2, Third Edition, doi: 10.1007/0-387-30742-7_13, 2006. 354-420, 2006.

Einsele, G., Yan, J. P., and Hinderer, M.: Atmospheric carbon burial in modern lake basins and its significance for the global carbon budget,
10 Global Planet Change, 30, 167-195, 2001.

Engstrom, D. R. and Wright Jr, H.: Chemical stratigraphy of lake sediments as a record of environmental change, Lake sediments and environmental history: studies in palaeolimnology and palaeoecology in honour of Winifred Tutin/edited by EY Haworth and JWG Lund, 1984. 1984.

Fischer, U. R. and Velimirov, B.: High control of bacterial production by viruses in a eutrophic oxbow lake, Aquat Microb Ecol, 27, 1-12,
15 2002.

Froelich, P. N., Klinkhammer, G. P., Bender, M. L., Luedtke, N. A., Heath, G. R., Cullen, D., Dauphin, P., Hammond, D., Hartman, B., and Maynard, V.: Early Oxidation of Organic-Matter in Pelagic Sediments of the Eastern Equatorial Atlantic - Suboxic Diagenesis, Geochim Cosmochim Ac, 43, 1075-1090, 1979.

Gachter, R. and Muller, B.: Why the phosphorus retention of lakes does not necessarily depend on the oxygen supply to their sediment
20 surface, Limnol Oceanogr, 48, 929-933, 2003.

Giles, C. D., Isles, P. D. F., Manley, T., Xu, Y. Y., Druschel, G. K., and Schroth, A. W.: The mobility of phosphorus, iron, and manganese through the sediment-water continuum of a shallow eutrophic freshwater lake under stratified and mixed water-column conditions, Biogeochemistry, 127, 15-34, 2016.

Gontikaki, E., Polymenakou, P. N., Thornton, B., Narayanaswamy, B. E., Black, K., Tselepides, A., and Witte, U.: Microbial Response to
25 Organic Matter Enrichment in the Oligotrophic Levantine Basin (Eastern Mediterranean), Geomicrobiol J, 29, 648-655, 2012.

Gorham, E., Lund, J. W. G., Sanger, J. E., and Dean, W. E.: Some Relationships between Algal Standing Crop, Water Chemistry, and Sediment Chemistry in English Lakes, Limnol Oceanogr, 19, 601-617, 1974.

Gruca-Rokosz, R.: Diffusive Fluxes of CH4 and CO2 at the Sediment-Overlying Water Interface in Reservoir Ecosystems, J Ecol Eng, 19, 158-164, 2018.

30 Haglund, A. L., Lantz, P., Tornblom, E., and Tranvik, L.: Depth distribution of active bacteria and bacterial activity in lake sediment, Fems Microbiol Ecol, 46, 31-38, 2003.

Heathcote, A. J. and Downing, J. A.: Impacts of Eutrophication on Carbon Burial in Freshwater Lakes in an Intensively Agricultural Landscape, Ecosystems, 15, 60-70, 2012.

Hebting, Y., Schaeffer, P., Behrens, A., Adam, P., Schmitt, G., Schneckenburger, P., Bernasconi, S. M., and Albrecht, P.: Biomarker
35 evidence for a major preservation pathway of sedimentary organic carbon, Science, 312, 1627-1631, 2006.

Hedges, J. I., Eglinton, G., Hatcher, P. G., Kirchman, D. L., Arnosti, C., Derenne, S., Evershed, R. P., Kogel-Knabner, I., de Leeuw, J. W., Littke, R., Michaelis, W., and Rullkotter, J.: The molecularly-uncharacterized component of nonliving organic matter in natural environments, Org Geochem, 31, 945-958, 2000.

Hoehler, T. M., Albert, D. B., Alperin, M. J., and Martens, C. S.: Acetogenesis from CO2 in an anoxic marine sediment, Limnol Oceanogr,
40 44, 662-667, 1999.

Hoehler, T. M., Alperin, M. J., Albert, D. B., and Martens, C. S.: Apparent minimum free energy requirements for methanogenic Archaea and sulfate-reducing bacteria in an anoxic marine sediment, Fems Microbiol Ecol, 38, 33-41, 2001.

Hoehler, T. M., Alperin, M. J., Albert, D. B., and Martens, C. S.: Thermodynamic control on hydrogen concentrations in anoxic sediments, Geochim Cosmochim Ac, 62, 1745-1756, 1998.

45 Holgerson, M. A. and Raymond, P. A.: Large contribution to inland water CO2 and CH4 emissions from very small ponds, Nat Geosci, 9, 222-U150, 2016.

Hyun, J. H., Kim, S. H., Mok, J. S., Cho, H., Lee, T., Vandieken, V., and Thamdrup, B.: Manganese and iron reduction dominate organic carbon oxidation in surface sediments of the deep Ulleung Basin, East Sea, Biogeosciences, 14, 941-958, 2017.

Jørgensen, B. B. and Kasten, S.: Sulfur cycling and methane oxidation. In: Marine geochemistry, Springer, 2006.

50 Katsev, S. and Crowe, S. A.: Organic carbon burial efficiencies in sediments: The power law of mineralization revisited, Geology, 43, 607-610, 2015.

Kluepfel, L., Keiluweit, M., Kleber, M., and Sander, M.: Redox Properties of Plant Biomass-Derived Black Carbon (Biochar), Environ Sci Technol, 48, 5601-5611, 2014.

Klupfel, L., Piepenbrock, A., Kappler, A., and Sander, M.: Humic substances as fully regenerable electron acceptors in recurrently anoxic
55 environments, Nat Geosci, 7, 195-200, 2014.

Kristensen, E.: Organic matter diagenesis at the oxic/anoxic interface in coastal marine sediments, with emphasis on the role of burrowing animals, Hydrobiologia, 426, 1-24, 2000.

Kristensen, E., Penha-Lopes, G., Delefosse, M., Valdemarsen, T., Quintana, C. O., and Banta, G. T.: What is bioturbation? The need for a precise definition for fauna in aquatic sciences, Mar Ecol Prog Ser, 446, 285-302, 2012.

5 Lalonde, K., Mucci, A., Ouellet, A., and Gelinas, Y.: Preservation of organic matter in sediments promoted by iron, Nature, 483, 198-200, 2012.

Lehman, J. T.: Reconstructing Rate of Accumulation of Lake Sediment - Effect of Sediment Focusing, Quaternary Res, 5, 541-550, 1975.

Lehmann, M. F., Bernasconi, S. M., Barbieri, A., and McKenzie, J. A.: Preservation of organic matter and alteration of its carbon and nitrogen isotope composition during simulated and in situ early sedimentary diagenesis, Geochim Cosmochim Ac, 66, 3573-3584, 2002.

10 Lever, M. A.: Functional gene surveys from ocean drilling expeditions a review and perspective, Fems Microbiol Ecol, 84, 1-23, 2013.

Lever, M. A. and Teske, A. P.: Diversity of Methane-Cycling Archaea in Hydrothermal Sediment Investigated by General and Group-Specific PCR Primers, Appl Environ Microb, 81, 1426-1441, 2015.

Liechti, P.: Der Zustand der Seen in der Schweiz, Bundesamt für Umwelt, Bern, 1994.

Liu, Y. Q., Conrad, R., Yao, T. D., Gleixner, G., and Claus, P.: Change of methane production pathway with sediment depth in a lake on the Tibetan plateau, Palaeogeogr Palaeocl, 474, 279-286, 2017.

15 Lotter, A.: The effect of eutrophication on diatom diversity: examples from six Swiss lakes, 2001. 2001.

Lotter, A. F.: The recent eutrophication of Baldeggersee (Switzerland) as assessed by fossil diatom assemblages, Holocene, 8, 395-405, 1998.

Lovley, D. R. and Goodwin, S.: Hydrogen Concentrations as an Indicator of the Predominant Terminal Electron-Accepting Reactions in Aquatic Sediments, Geochim Cosmochim Ac, 52, 2993-3003, 1988.

20 Lovley, D. R. and Phillips, E. J. P.: Rapid Assay for Microbially Reducible Ferric Iron in Aquatic Sediments, Appl Environ Microb, 53, 1536-1540, 1987.

Maerki, M., Muller, B., Dinkel, C., and Wehrli, B.: Mineralization pathways in lake sediments with different oxygen and organic carbon supply, Limnol Oceanogr, 54, 428-438, 2009.

25 Maerki, M., Wehrli, B., Dinkel, C., and Muller, B.: The influence of tortuosity on molecular diffusion in freshwater sediments of high porosity, Geochim Cosmochim Ac, 68, 1519-1528, 2004.

McGlathery, K. J.: Macroalgal blooms contribute to the decline of seagrass in nutrient-enriched coastal waters, J Phycol, 37, 453-456, 2001.

Meals, D. W., Dressing, S. A., and Davenport, T. E.: Lag Time in Water Quality Response to Best Management Practices: A Review, J Environ Qual, 39, 85-96, 2010.

30 Mendonca, R., Muller, R. A., Clow, D., Verpoorter, C., Raymond, P., Tranvik, L. J., and Sobek, S.: Organic carbon burial in global lakes and reservoirs, Nat Commun, 8, 2017.

Meysman, F. J. R., Middelburg, J. J., and Heip, C. H. R.: Bioturbation: a fresh look at Darwin's last idea, Trends Ecol Evol, 21, 688-695, 2006.

Middelburg, J. J.: Reviews and syntheses: to the bottom of carbon processing at the seafloor, Biogeosciences, 15, 413-427, 2018.

35 Moosmann, L., Gachter, R., Muller, B., and Wuest, A.: Is phosphorus retention in autochthonous lake sediments controlled by oxygen or phosphorus?, Limnol Oceanogr, 51, 763-771, 2006.

Müller, G., Ehwald, F., and Hamann, A.: Langzeituntersuchungen über das Verhalten von Phosphor, Stickstoff und Bor bei der mechanisch-biologischen Abwasserreinigung am Beispiel der kommunalen Kläranlagen Bammental und Wiesloch (Rhein-Neckar-Kreis), Univ. Heidelberg, Heidelberg, 1990.

40 Naeher, S., Gilli, A., North, R. P., Hamann, Y., and Schubert, C. J.: Tracing bottom water oxygenation with sedimentary Mn/Fe ratios in Lake Zurich, Switzerland, Chem Geol, 352, 125-133, 2013.

Nedwell, D. B.: The Input and Mineralization of Organic-Carbon in Anaerobic Aquatic Sediments, Adv Microb Ecol, 7, 93-131, 1984.

Oda, Y., Larimer, F. W., Chain, P. S. G., Malfatti, S., Shin, M. V., Vergez, L. M., Hauser, L., Land, M. L., Braatsch, S., Beatty, J. T., Pelletier, D. A., Schaefer, A. L., and Harwood, C. S.: Multiple genome sequences reveal adaptations of a phototrophic bacterium to sediment microenvironments, P Natl Acad Sci USA, 105, 18543-18548, 2008.

45 Oremland, R. S. and Polcin, S.: Methanogenesis and Sulfate Reduction - Competitive and Noncompetitive Substrates in Estuarine Sediments, Appl Environ Microb, 44, 1270-1276, 1982.

Pritchard, P. H. and Bourquin, A. W.: The Use of Microcosms for Evaluation of Interactions between Pollutants and Microorganisms, Adv Microb Ecol, 7, 133-215, 1984.

50 Raymond, P. A., Hartmann, J., Lauerwald, R., Sobek, S., McDonald, C., Hoover, M., Butman, D., Striegl, R., Mayorga, E., Humborg, C., Kortelainen, P., Durr, H., Meybeck, M., Ciais, P., and Guth, P.: Global carbon dioxide emissions from inland waters, Nature, 503, 355-359, 2013.

Rippey, B. and Anderson, N. J.: Reconstruction of lake phosphorus loading and dynamics using the sedimentary record, Environ Sci Technol, 30, 1786-1788, 1996.

55 Sander, M., Hofstetter, T. B., and Gorski, C. A.: Electrochemical Analyses of Redox-Active Iron Minerals: A Review of Nonmediated and Mediated Approaches, Environ Sci Technol, 49, 5862-5878, 2015.

Schaller, T. and Wehrli, B.: Geochemical-Focusing of Manganese in Lake Sediments - An Indicator of Deep-Water Oxygen Conditions, Aquat Geochem, 2, 359-378, 1996.

Schindler, D. W.: Recent advances in the understanding and management of eutrophication, Limnol Oceanogr, 51, 356-363, 2006.

Schink, B.: Energetics of syntrophic cooperation in methanogenic degradation, Microbiol Mol Biol R, 61, 262-+, 1997.

5 Schwarz, J. I. K., Eckert, W., and Conrad, R.: Community structure of Archaea and Bacteria in a profundal lake sediment Lake Kinneret (Israel), Syst Appl Microbiol, 30, 239-254, 2007.

Sobek, S., Durisch-Kaiser, E., Zurbrugg, R., Wongfun, N., Wessels, M., Pasche, N., and Wehrli, B.: Organic carbon burial efficiency in lake sediments controlled by oxygen exposure time and sediment source, Limnol Oceanogr, 54, 2243-2254, 2009.

Stadelmann, P. and Escher, M.: 20 Jahre Sanierung und Ueberwachung des Baldeggersees, Naturforschende Gesellschaft, Luzern, 2002.

10 Steinsberger, T., Schmid, M., Wuest, A., Schwefel, R., Wehrli, B., and Muller, B.: Organic carbon mass accumulation rate regulates the flux of reduced substances from the sediments of deep lakes, Biogeosciences, 14, 3275-3285, 2017.

Stookey, L. L.: Ferrozine - a New Spectrophotometric Reagent for Iron, Anal Chem, 42, 779-&, 1970.

Teranes, J. L. and Bernasconi, S. M.: The record of nitrate utilization and productivity limitation provided by delta N-15 values in lake organic matter - A study of sediment trap and core sediments from Baldeggersee, Switzerland, Limnol Oceanogr, 45, 801-813, 2000.

15 Teranes, J. L., McKenzie, J. A., Bernasconi, S. M., Lotter, A. F., and Sturm, M.: A study of oxygen isotopic fractionation during bio-induced calcite precipitation in eutrophic Baldeggersee, Switzerland, Geochim Cosmochim Ac, 63, 1981-1989, 1999a.

Teranes, J. L., McKenzie, J. A., and Lotter, A. F.: Stable isotope response to lake eutrophication: Calibration of a high-resolution lacustrine sequence from Baldeggersee, Limnol Oceanogr, 44, 320-333, 1999b.

Valiela, I., McClelland, J., Hauxwell, J., Behr, P. J., Hersh, D., and Foreman, K.: Macroalgal blooms in shallow estuaries: Controls and 20 ecophysiological and ecosystem consequences, Limnol Oceanogr, 42, 1105-1118, 1997.

Werne, J. P., Hollander, D. J., Behrens, A., Schaeffer, P., Albrecht, P., and Damste, J. S. S.: Timing of early diagenetic sulfurization of organic matter: A precursor-product relationship in Holocene sediments of the anoxic Cariaco Basin, Venezuela, Geochim Cosmochim Ac, 64, 1741-1751, 2000.

Werne, J. P., Lyons, T. W., Hollander, D. J., Schouten, S., Hopmans, E. C., and Damste, J. S. S.: Investigating pathways of diagenetic 25 organic matter sulfurization using compound-specific sulfur isotope analysis, Geochim Cosmochim Ac, 72, 3489-3502, 2008.

Witherspoon, P. A. and Saraf, D. N.: Diffusion of Methane Ethane Propane and N-Butane in Water from 25 to 43 Degrees, J Phys Chem-Us, 69, 3752-+, 1965.

Xiao, K. Q., Beulig, F., Kjeldsen, K. U., Jorgensen, B. B., and Risgaard-Petersen, N.: Concurrent Methane Production and Oxidation in Surface Sediment from Aarhus Bay, Denmark, Front Microbiol, 8, 2017.

30 Zeebe, R. E.: On the molecular diffusion coefficients of dissolved CO_2, HCO_3^-, and CO_3^{2-} and their dependence on isotopic mass, Geochim Cosmochim Ac, 75, 2483-2498, 2011.
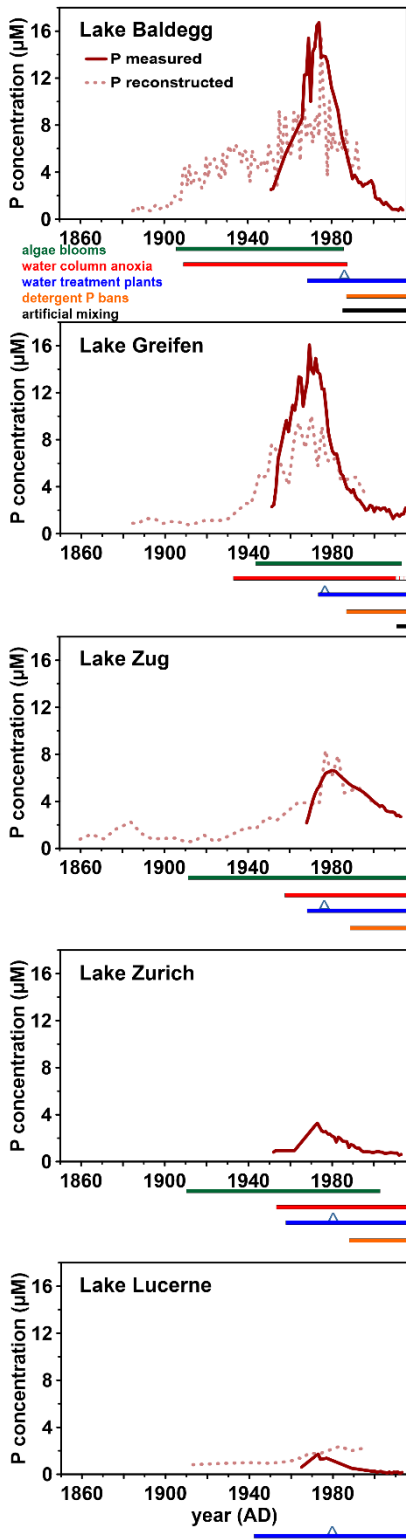
Figure 1: Historical data on surface water P concentrations and eutrophication since 1860. P concentration monitoring was started between 1950 and 1970. Reconstructed P concentrations were modelled based on sedimentary records of diatom assemblages. Below each graph, timelines of algae bloom and anoxic event occurrence, wastewater treatment, and artificial mixing are shown. P bans were implemented in 1986 and are marked by blue triangles. All data from Swiss Federal Office of the Environment (BAFU, 2013), except reconstructed P concentrations (Lake Lucerne: Lotter (2001); Lake Baldegg: Lotter (1998); Lake Zug: Aquaplus (Elber et al. (2001); Lake Greifen: Aquaplus (Elber et al. (2004); no data exist for Lake Zurich)).
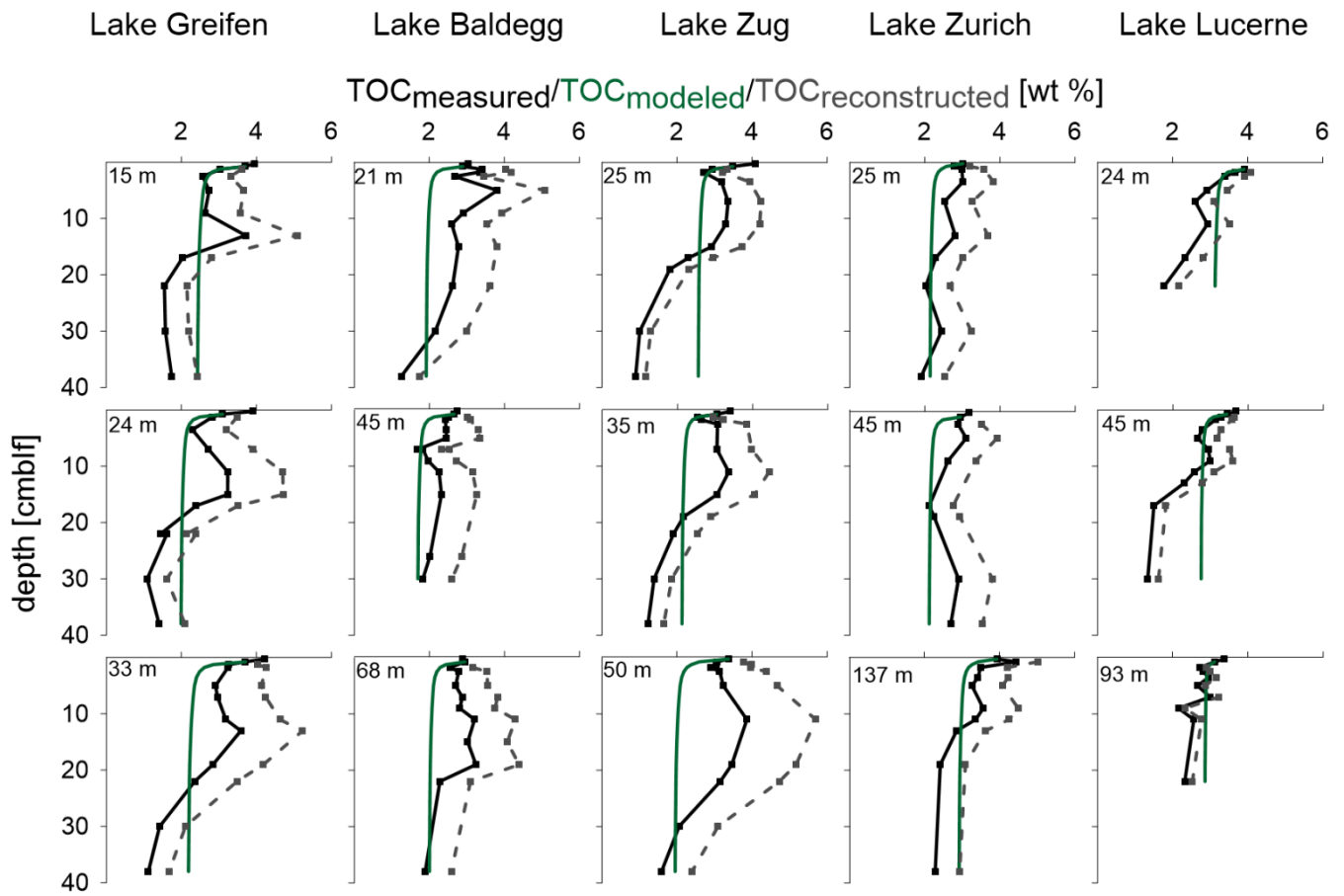
Figure 2: TOC (solid black line), TOC_modeled (solid green line), and TOC_reconstructed (grey dashed line). Water depth [m] for each station is indicated at the top of each subplot; cmblf = cm below lake floor.
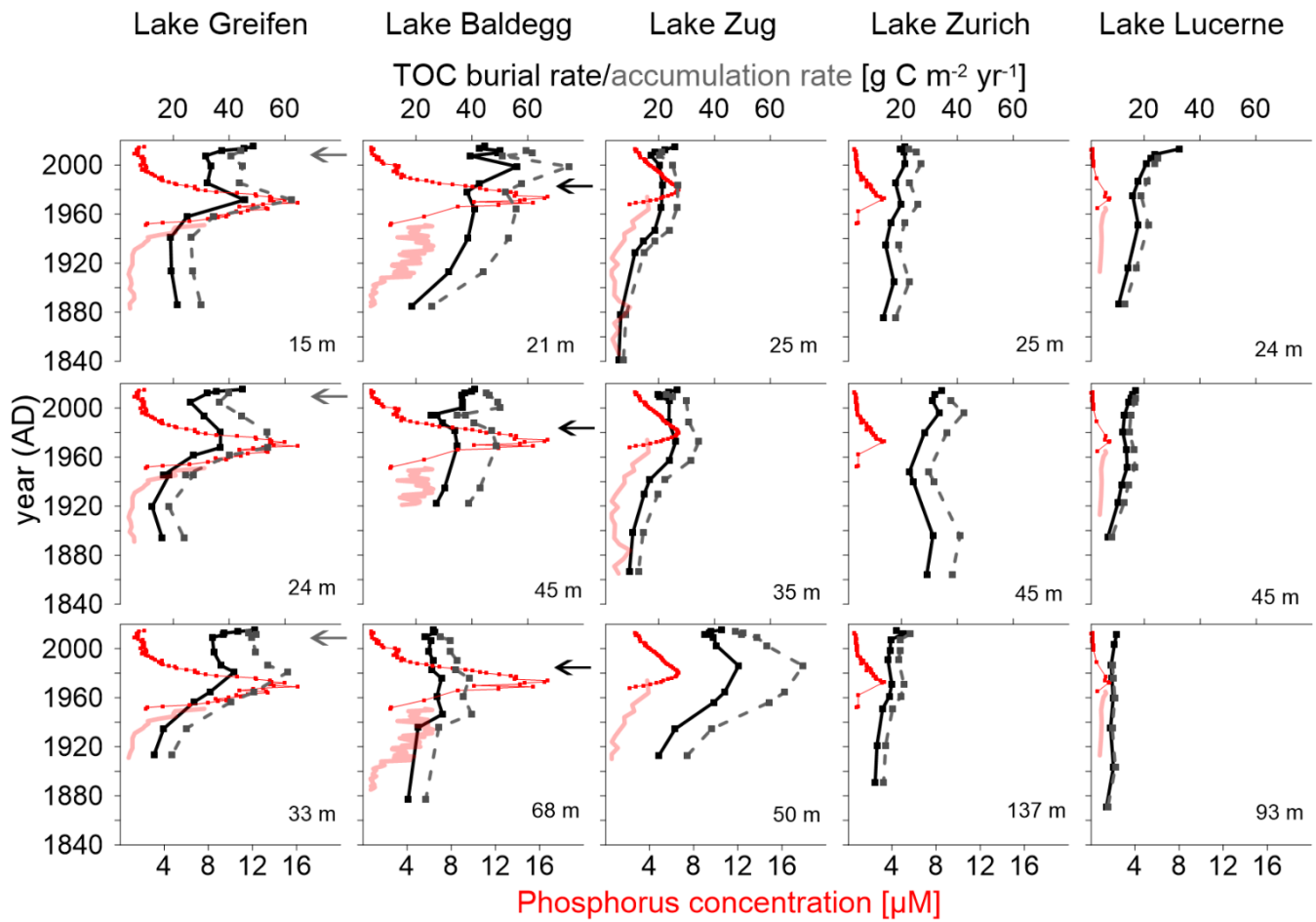
Figure 3: TOC burial rates (black solid lines), reconstructed TOC accumulation rates (dashed grey lines), measured water column total P concentrations (red solid lines), and reconstructed water column total P concentrations (red-dotted lines) all plotted against sediment age at various lakes and lake stations.
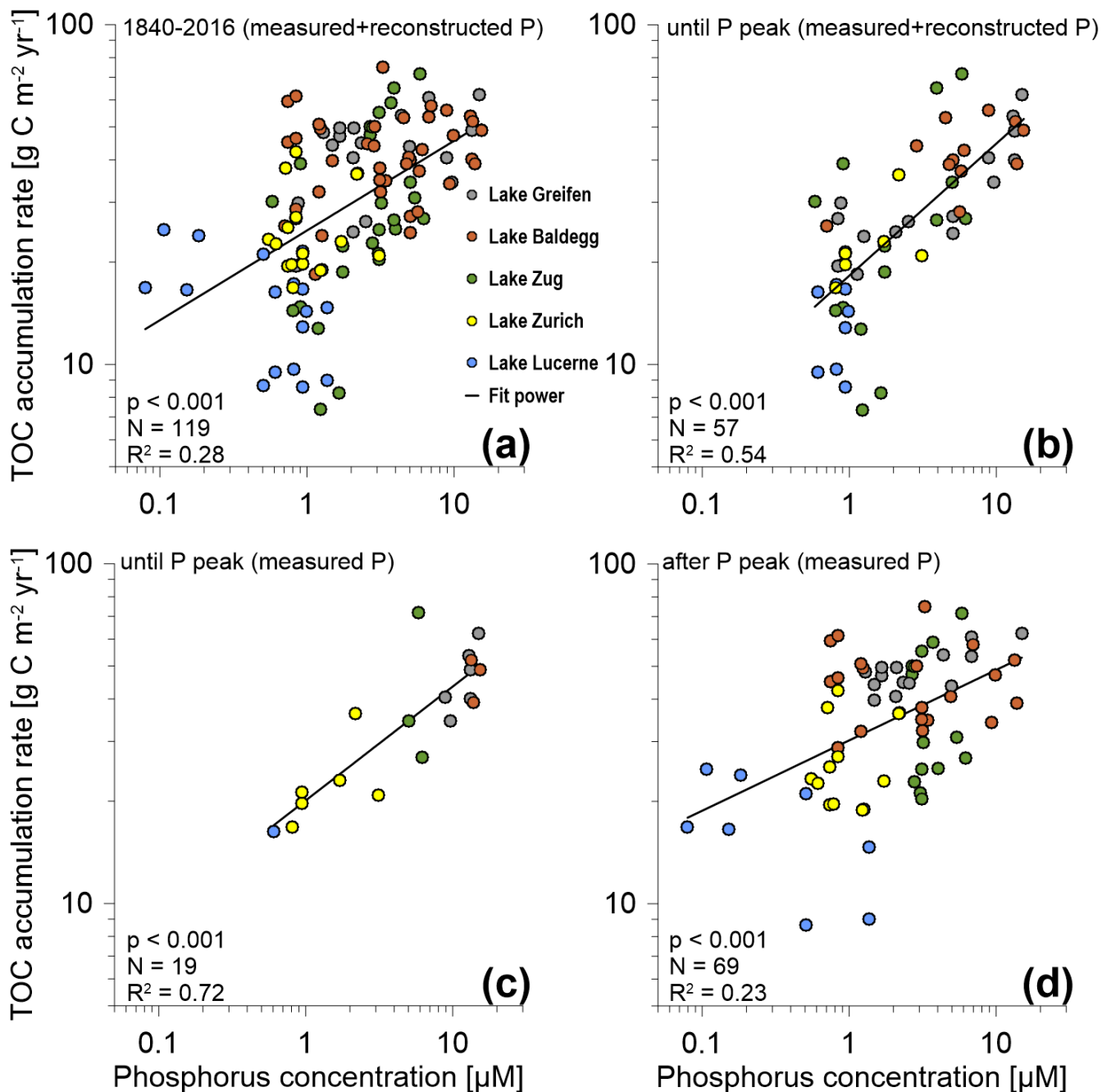
Figure 4: TOC accumulation rates [g C m^{-2} yr^{-1}] vs. P concentrations for (a) the entire P dataset (1840-2016), (b) measured and reconstructed P concentrations until the P concentration peak in the 1960s and 1970s (includes the peak), (c) only measured P concentrations for the time period until the P concentration peak (includes the peak), and (d) measured P concentrations for the time period after the P concentration peak. N is the number of data points included in each graph. Coefficients of determination (R^2) values are based on best-fit Power trendlines. P-values are based on two-sided Spearman Rank Correlation tests. [Note: for Lake Zurich, only measured P data were available. Furthermore, in (a) and (b), for data points where both measured and reconstructed P concentrations were available, we only included measured values.]
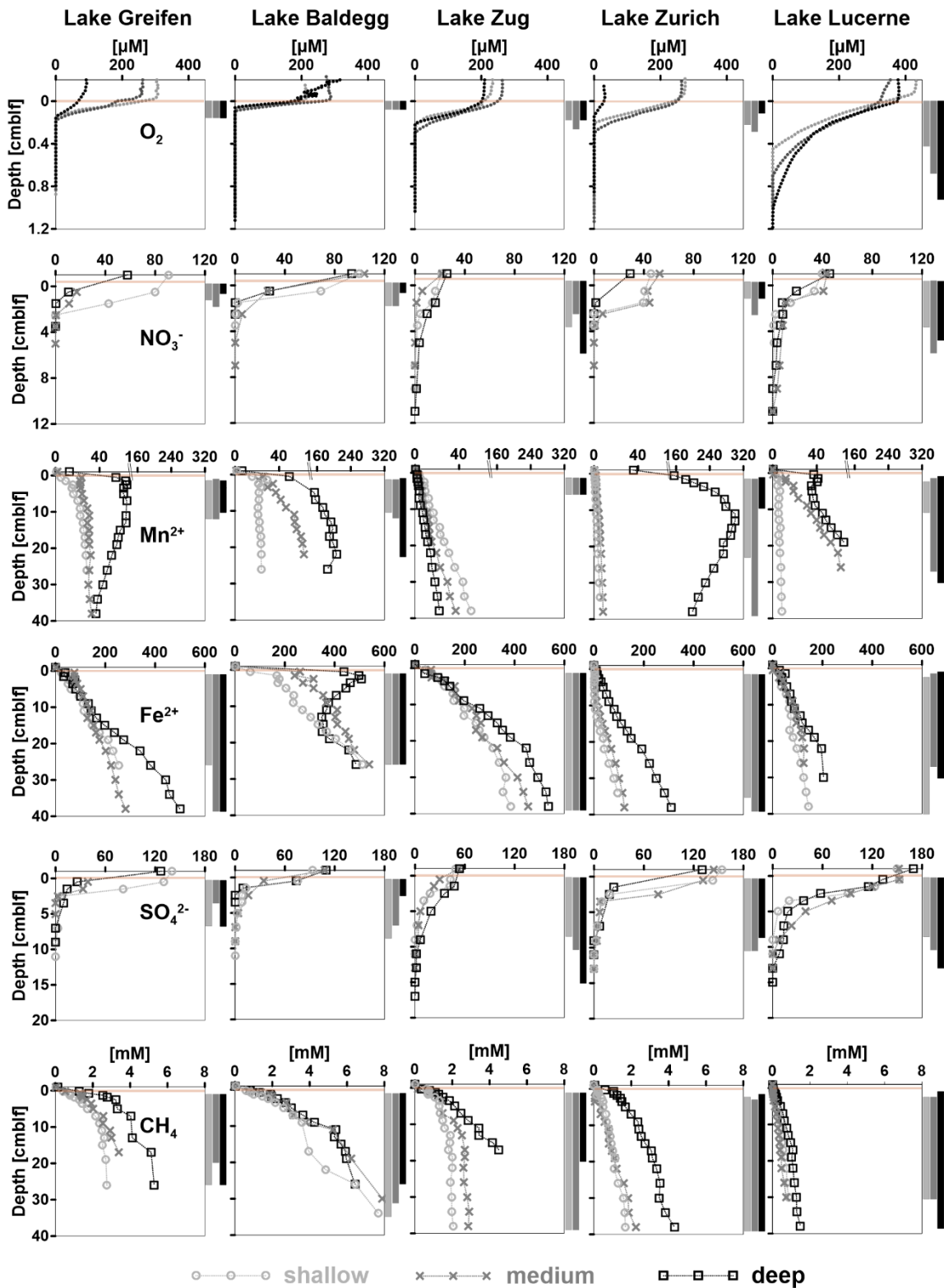
Figure 5: Concentration profiles of O_2, NO_3^-, Mn^{2+}, Fe^{2+}, SO_4^{2-}, and CH_4 vs. sediment depth (cmblf) organized by analyte and lake. Each graph shows concentration profiles of all three stations per lake. Light brown horizontal bars indicate the depth of the sediment-water-interface. CH_4 measurements with significant outgassing during sampling were omitted. The inferred depth distributions of respiration reactions are indicated by vertical bars to the right of each graph. Notes: (1) depth ranges on y-axes vary between analytes; (2) analyte concentration ranges on x-axes vary with analytes (3) Please not there is no BW sample available for SO_4^{2-} and NO_3^- at Lake Greifen medium station.
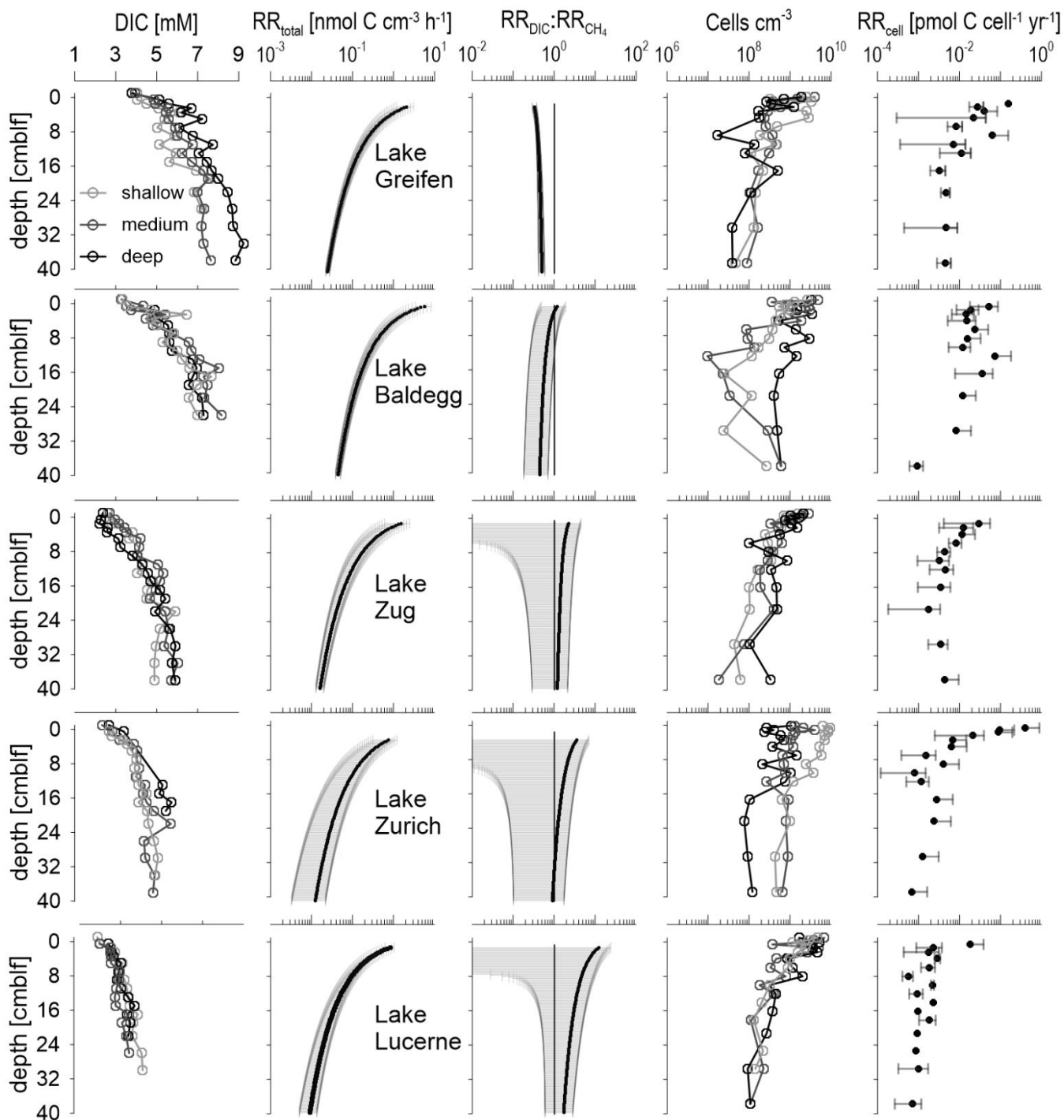
Figure 6: Depth profiles of DIC concentrations, total microbial respiration rates ($RR_{total} = RR_{DIC} + RR_{CH4}$), ratios of DIC production to methanogenesis rates ($RR_{DIC}:RR_{CH4}$), cell abundances, and cell-specific respiration rates (RR_{cell}). DIC concentrations and cell counts are shown for each station individually. RR_{total} and $RRt_{otal}:RR_{CH4}$ are lake-specific averages (black line) with standard deviation ranges (grey areas). A 1:1 line indicates $RR_{DIC} = RR_{CH4}$. RR_{cell} are averages±SD for samples with cell count data.
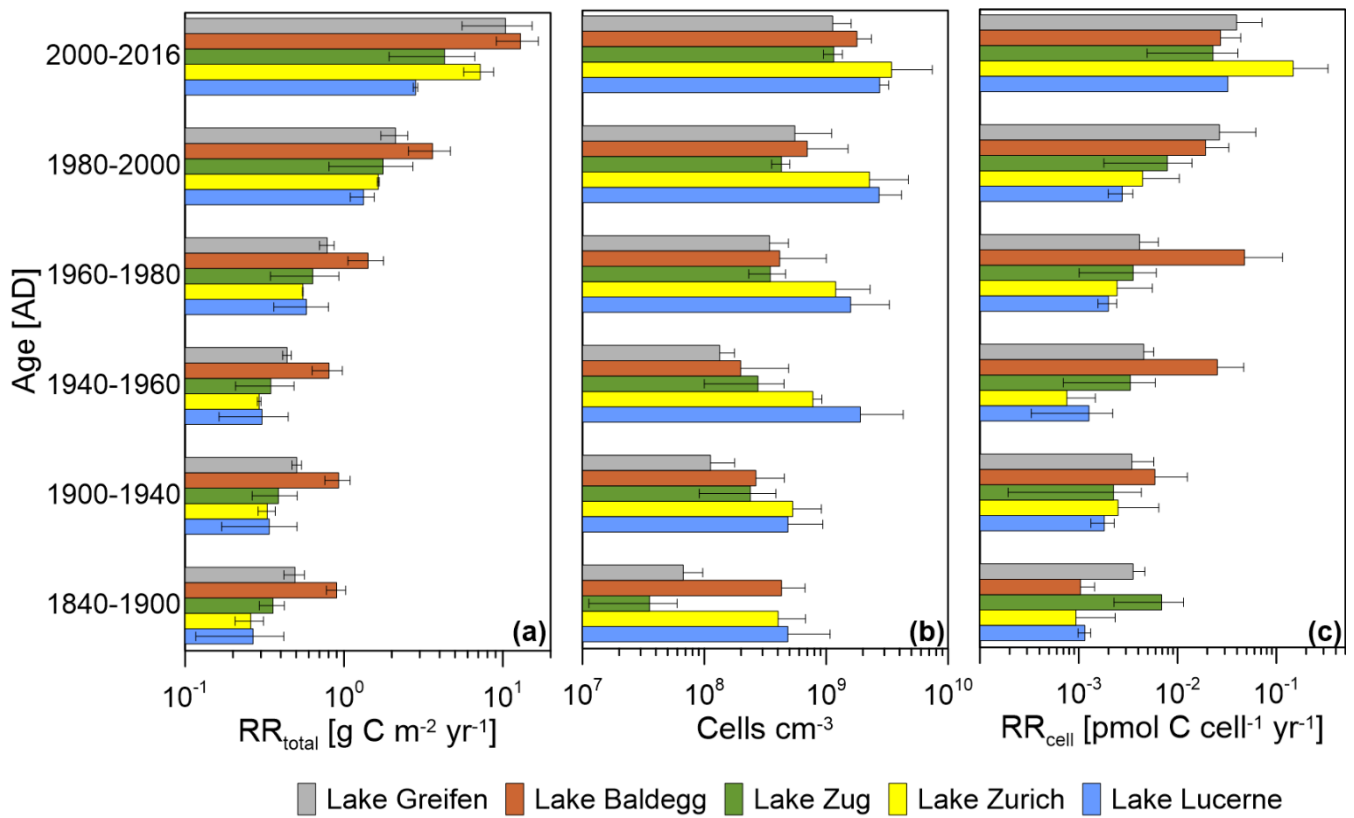
Figure 7: Relationships between RR$_{total}$, microbial abundance, and RR$_{cell}$ and sediment age. Error bars indicate standard deviations of averages for the three stations per lake during each time interval.

Table 1: Overview of sampled lakes, their trophic status, and maximum water depths (from BAFU 2012, 2013), as well as the geographic coordinates, water depths, and bottom water dissolved O_2 concentrations of the stations that were sampled. O_2 concentrations ≤15.6 µM are termed 'hypoxic'.

	Trophic status	Max. depth (m)	Station #	Latitude (°N)	Longitude (°E)	Water depth (m)	O_2 (µM)
Lake Greifen	eutrophic	32	1	47° 21.134	8° 40.511	15	seasonally hypoxic
			2	47° 21.118	8° 40.484	32	
			3	47° 21.038	8° 40.185	24	
Lake Baldegg	eutrophic	66	1	47° 11.929	8° 15.613	66	15.6–125
			2	47° 11.759	8° 15.392	45	125–250
			3	47° 11.649	8° 15.417	21	15.6–125
Lake Zug	eutrophic	198	1	47° 10.272	8° 30.036	25	125–250
			2	47° 10.104	8° 29.946	35	125–250
			3	47° 09.834	8° 29.814	50	125–250
Lake Zurich	mesotrophic	137	1	47° 16.995	8° 35.624	137	hypoxic
			2	47° 16.708	8° 35.033	45	125–250
			3	47° 16.395	8° 35.195	25	15.6–125
Lake Lucerne	oligotrophic	214	1	47° 00.051	8° 20.218	24	>250
			2	46° 59.812	8° 20.820	93	>250
			3	46° 59.915	8° 20.413	45	>250

Table 2: Sedimentation rates, depth distributions of laminated layers, bottom water temperature, porewater pH, and average % TOC (± standard deviation (SD); 1920–2016) across stations in each lake. Triangles indicate laminations with the presence of turbidites. Stars indicate sediments without clear ^{137}Cs peaks. Sedimentation rates changed in Lake Zurich (25 m), from 0.23 cm yr^{-1} in the top 7 cm to 0.27 cm yr^{-1} below, and in Lake Lucerne (45 m) from 0.16 cm yr^{-1} in the top 5 cm to 0.14 cm yr^{-1} below.

	Station (water depth in m)	Sed. rate (cm yr^{-1})	Yearly lamination intervals (cm)	Temperature (°C)	PW pH ranges	TOC [wt %]
Lake Greifen	shallow (15 m)	0.29	10–17	7	7.29–7.75	2.9 (± 0.8)
	medium (24 m)	0.31	2–21	7	7.18–7.88	2.5 (± 0.9)
	deep (33 m)	0.37	2–35	6	7.21–7.46	3.1 (± 0.7)
Lake Baldegg	shallow (21 m)	0.29 (*)	11–13	7	7.37–8.38	3.0 (± 0.4)
	medium (45 m)	0.32 (*)	20–30	7	7.35–8.30	2.2 (± 0.3)
	deep (68 m)	0.27	7–40	7	7.54–8.15	2.8 (± 0.3)
Lake Zug	shallow (25 m)	0.22	no	7	7.46–7.82	3.0 (± 0.6)
	medium (35 m)	0.25	no	7	7.41–8.00	2.8 (± 0.5)
	deep (50 m)	0.37	no	7	7.37–8.02	3.1 (± 0.5)
Lake Zurich	shallow (25 m)	0.23/0.27	no	7	7.38–8.07	2.7 (± 0.4)
	medium (45 m)	0.35 (*)	20–35	7	7.50–8.08	2.7 (± 0.4)
	deep (137 m)	0.2	0–20$^\Delta$, 26–28$^\Delta$, 37–38$^\Delta$	6	7.18–8.01	3.4 (± 0.6)
Lake Lucerne	shallow (24 m)	0.17	no	9	7.40–7.70	3.4 (± 0.9)
	medium (45 m)	0.16/0.14	no	7	7.38–7.84	3.0 (± 0.4)
	deep (93 m)	0.06	no	5	7.42–7.84	2.9 (± 0.3)

Table 3: Average ± SD depth distributions (cmblf) of microbial respiration reactions in each lake.

	Greifen	Baldegg	Zug	Zurich	Lucerne
Aerobic	surface – 0.17±0.03	surface – 0.08±0.02	surface – 0.23±0.03	surface – 0.22±0.08	surface – 0.73±0.25
Denitrification	surface – 2.5±1.0	surface – 2.8±1.2	surface – 7.7±3.1	surface – 3.3±1.4	surface – 9±2.0
Mn reduction	0.3±0.3 – 8.2± 4.9	0.3±0.3 – 14.0±7.0	0.5±0.0 – 5.0±0.0	0.3±0.3 – 24.0±15.1	0.7±0.8 – bottom
Fe reduction	0.5 ±0.0 – bottom	throughout	0.5±0.0 – bottom	0.5±0.0 – bottom	0.8±0.6 – bottom
Sulfate reduction	surface – 5.8±2.0	surface – 6.2±3.3	surface – 11.7±3.1	surface – 10.3±1.2	surface – 11.0±2.0
Methanogenesis	surface – bottom	surface – bottom	surface – bottom	2.6±2.4 – bottom	3.0±1.7 – bottom